D4.3 Conceptual design and techno-economic feasibility study

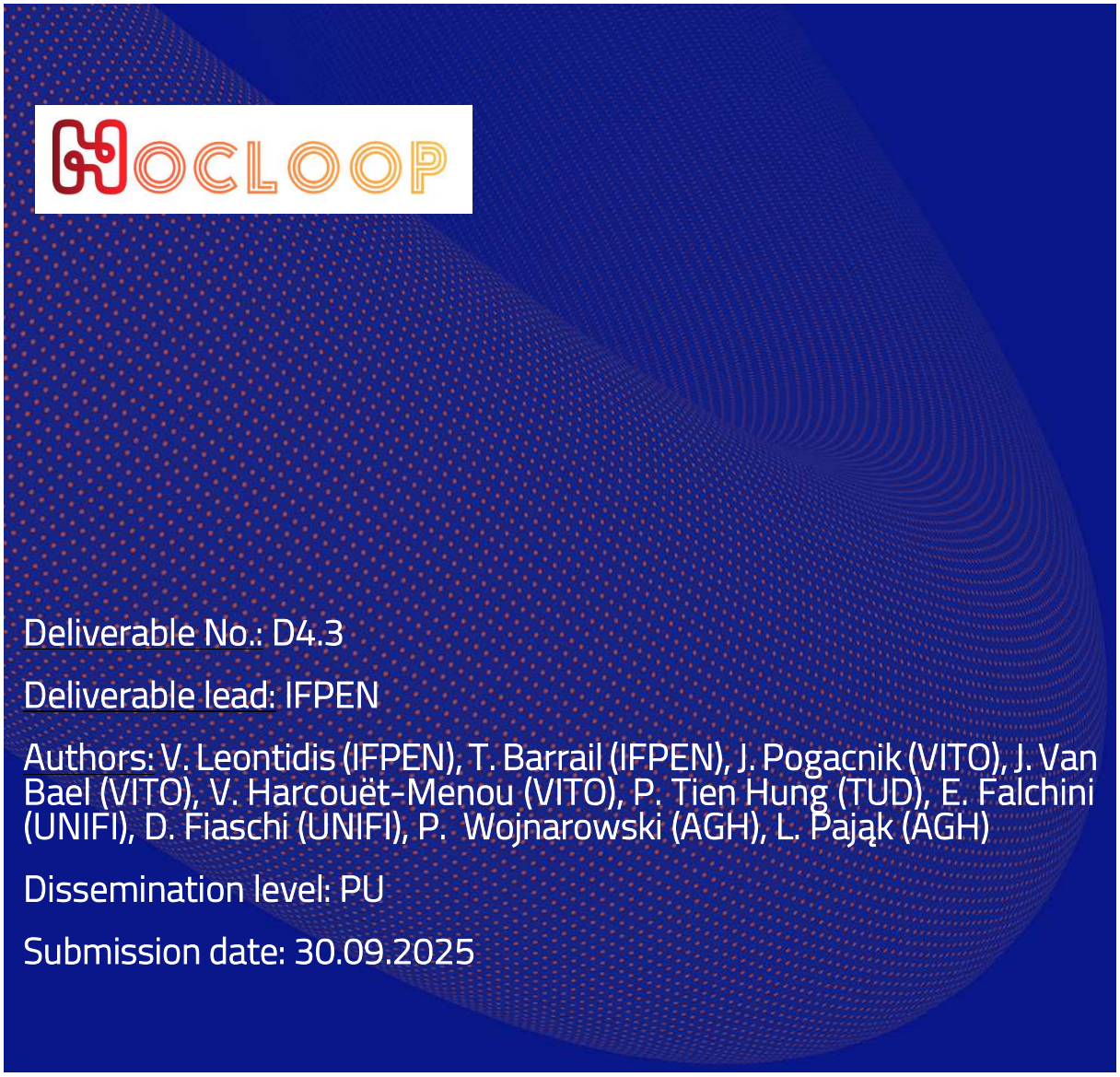

Deliverable No.: D4.3

Deliverable lead: IFPEN

Authors: V. Leontidis (IFPEN), T. Barrail (IFPEN), J. Pogacnik (VITO), J. Van Bael (VITO), V. Harcouët-Menou (VITO), P. Tien Hung (TUD), E. Falchini (UNIFI), D. Fiaschi (UNIFI), P. Wojnarowski (AGH), L. Pająk (AGH)

Dissemination level: PU

Submission date: 30.09.2025

Funded by the European Union. Views and opinions expressed are however those of the author(s) only and do not necessarily reflect those of the European Union or CINEA. Neither the European Union nor the granting authority can be held responsible for them.

PROJECT INFORMATION

PROJECT ACRONYM	HOCLOOP
Call ID	HORIZON- CL5-2021-D3-03-15
Project title	A circular by design environmentally friendly geothermal energy solution based on a horizontal closed loop - HOCLOOP
Grant Agreement No	101083558
Start of Project	01.10.2022
Project Duration	42 Months
Type of Action	HORIZON Research and Innovation Actions
Coordinator	IFE

DOCUMENT INFORMATION

Deliverable No.	D4.3
Work Package	WP4
Deliverable Lead	IFPEN
Deliverable Authors	V. Leontidis (IFPEN), T. Barrail (IFPEN), J. Pogacnik (VITO), J. Van Bael (VITO), V. Harcouët-Menou (VITO), P. Tien Hung (TUD), E. Falchini (UNIFI), D. Fiaschi (UNIFI), P. Wojnarowski (AGH), L. Pająk (AGH)
Issue	1/1
Due date	30.09.2025
Submission date	30.09.2025
Dissemination level[1]	PU

[1] Dissemination level: **PU** = Public, **SEN** = Sensitive, **R-UE/EU-R** = EU classified, **C-UE/EU-C** = EU classified, **S-UE/EU-S** – EU classified

This project has received funding from the European Union's Horizon Europe research and innovation program under grant agreement No 101083558

Nature[2]	R
Copyright	© 2023 Consortium

DOCUMENT HISTORY

DATE	VERSION	MODIFIED BY	COMMENT
15.09.2025	0.1	V. Leontidis (IFPEN), T. Barrail (IFPEN), J. Pogacnik (VITO), J. Van Bael (VITO), V. Harcouët-Menou (VITO), P. Tien Hung (TUD), E. Falchini (UNIFI), D. Fiaschi (UNIFI), P. Wojnarowski (AGH), L. Pająk (AGH)	First draft for internal revision
17.09.2025	0.2	Mario Silva (IFE)	First internal revision
17.09.2025	0.3	Mario Silva (IFE)	Distributed for peer review
24.09.2025 30.09.2025	0.4	Steinar Lomeland (NORCE) Magnus Wangen (IFE)	Reviewer's comments
30.09.2025	1.0	Mario Silva (IFE)	Review addressed
30.09.2025	2.0	Mario Silva (IFE)	Final version

[2] Nature of the deliverable: deliverable: **R** = Document, report; **DEM** – Demonstrator, pilot, prototype; **DEC** – Websites, patent, filings, videos etc; **DATA** – data sets, microdata, etc; **DMP** – Data Management Plan; **ETHICS**; **SECURITY**; **OTHER**

This project has received funding from the European Union's Horizon Europe research and innovation program under grant agreement No 101083558

TABLE OF CONTENT

This project has received funding from the European Union's Horizon Europe research and innovation program under grant agreement No 101083558

This project has received funding from the European Union's Horizon Europe research and innovation program under grant agreement No 101083558

LIST OF TABLES

This project has received funding from the European Union's Horizon Europe research and innovation program under grant agreement No 101083558

LIST OF FIGURES

This project has received funding from the European Union's Horizon Europe research and innovation program under grant agreement No 101083558

This project has received funding from the European Union's Horizon Europe research and innovation program under grant agreement No 101083558

LIST OF ABBREVATIONS

ACRONYM	DESCRIPTION
ATES	Aquifer Thermal Energy Storage
BHE	Borehole Heat Exchangers
CAPEX	Capital Expenditure
CEPCI	Chemical Engineering Plant Cost Index
CF	Capacity Factor
CHP	Combined Heat and Power
DHN	District Heating Network
DHS	Dual Heat String
DEX	Direct Heat Exchanger
EGS	Enhanced Geothermal Systems
HE	Heat Exchanger
HOCI	Hot Outlet Cold Inlet
ID	Inner Diameter
ISBL	Inside Battery Limits
KPI	Key Performance Indicator
LCOE	Levelized Cost of Energy
MD-BTES	Medium-Deep Borehole Thermal Energy Storage
OD	Outer Diameter
OPEX	Operational Expenditure
ORC	Organic Rankine Cycle
OSBL	Outside Battery Limits
P&ID	Piping and Instrumentation Diagrams
PPR	Polypropylene
PUO	Python Unit Operation
TMY	Typical Meteorological Year
TVD	True Vertical Depth

This project has received funding from the European Union's Horizon Europe research and innovation program under grant agreement No 101083558

EXECUTIVE SUMMARY

Scope of the deliverable

The objective of WP4 is to advance the HOCLOOP concept towards commercial deployment through comprehensive techno-economic feasibility studies at selected pilot sites. Task 4.3 focuses on developing conceptual pre-designs for both underground and surface energy systems, conducting detailed energy flow simulations, and performing economic analyses for each pilot location. This deliverable presents integrated technical and economic assessments of the HOCLOOP system implementation across five European pilot sites: France (Fresnes), Belgium (Mol), Germany (Darmstadt), Italy, and Poland (Goleniów). The work builds upon the geological characterization from D4.1 [1] and the underground simulations from D4.2 [2] to evaluate the commercial viability of site-specific HOCLOOP deployments.

Main conclusions

The techno-economic analysis reveals significant variability in the economic viability of HOCLOOP systems across different geological and market contexts. The French case study demonstrates a levelized cost of energy (LCOE) of 0.379 €/kWh, which remains substantially higher than conventional energy sources due to the dominance of drilling costs in the capital structure. The Belgian case shows more promise with an estimated investment of 2.3 M€ for well completion and 0.3-0.4 M€ for surface infrastructure, offering a technically feasible solution for heating new office buildings with a LCOE of 0.152 €/kWh. The German case indicates that while HOCLOOP's dual-pipe technology offers technical advantages, the low temperature gradient and high drilling costs in crystalline rock make it economically uncompetitive compared to existing solutions. The Italian cases indicate that competitive a LCOE (0.07763-0.09622 €/kWh for the Amiata case) can be obtained if the drilling conditions and the geothermal gradient are favorable, otherwise the dominance of the drilling cost in the capital investment can lead to much higher values (LCOE = 0.2688 €/kWh for the Gavorrano Case). The Polish case, despite favorable geological conditions in salt structures, requires substantial subsidies (40-60% of capital costs) to achieve economic viability within a 30-year operational period, with energy costs ranging from 0.052 to 0.129 €/GJ depending on the integration scenario. These findings underscore that HOCLOOP deployment requires careful site selection prioritizing high geothermal gradients, favorable drilling conditions, and integration opportunities with existing infrastructure to approach economic competitiveness.

This project has received funding from the European Union's Horizon Europe research and innovation program under grant agreement No 101083558

1. Introduction

The HOCLOOP project represents an innovative approach to geothermal energy extraction through horizontal closed-loop systems, addressing key challenges in sustainable heat production across diverse European geological settings. Building upon the comprehensive data collection and characterization completed in Task 4.1 (D4.1) [1]and the underground simulation results from Task 4.2 (D4.2) [2], this deliverable presents the culmination of techno-economic feasibility assessments for the HOCLOOP concept at five strategically selected pilot sites.

The primary objective of Task 4.3 is to develop conceptual pre-designs that integrate both underground loop configurations and above-ground energy systems, tailored to the specific geological, thermal, and economic conditions at each pilot location. Based on these designs, detailed energy flow simulations are performed to calculate key performance indicators (KPIs) defined in Tasks 5.1 [3] and 5.2 [4], enabling a comprehensive multi-criteria analysis for selecting the most promising configurations. The selected pre-designs are then elaborated to include preliminary piping and instrumentation diagrams (P&ID), along with detailed capital expenditure (CAPEX) and operational expenditure (OPEX) estimations.

This deliverable addresses critical questions regarding the economic viability of HOCLOOP systems in various European contexts, examining integration possibilities with existing district heating networks, evaluating temperature and flow constraints, and assessing the potential impact on local energy systems. The analysis considers current energy market conditions, including carbon pricing mechanisms, renewable energy incentives, and competing technologies, to provide a realistic assessment of HOCLOOP's commercial potential.

The work presented here directly supports the HOCLOOP project's overarching goal of developing a scalable, environmentally sustainable geothermal solution that can contribute to Europe's decarbonization objectives while providing economically viable alternatives to fossil fuel-based heating systems.

This project has received funding from the European Union's Horizon Europe research and innovation program under grant agreement No 101083558

2. Methodology

The techno-economic feasibility assessment follows a systematic approach combining technical simulation with economic modelling to evaluate HOCLOOP implementation at each pilot site. The methodology consists of four integrated components:

Technical Design and Integration Analysis

For each pilot site, conceptual designs were developed based on local geological conditions, existing infrastructure, and energy demand profiles. The design process incorporated well trajectory optimization from D4.2, surface equipment sizing, and integration strategies with existing or planned district heating networks.

Energy System Modelling

Dynamic energy simulations were performed using validated tools from WP2, including GTW for subsurface heat extraction and specialized surface equipment models. For sites with existing geothermal installations, comparative analyses were conducted between HOCLOOP and conventional systems. Operational parameters such as flow rates, injection temperatures, and pressure drops were optimized to maximize thermal output while maintaining system stability over projected operational lifetimes of 20-30 years.

Economic Analysis Framework

Cost estimations followed industry-standard methodologies, incorporating drilling costs based on local market conditions and well depths, equipment costs, vendor quotations, and installation costs including mobilization, site preparation, and commissioning. The scope and level of refinement of the economic assessment varied across sites: in certain cases, comprehensive financial models were constructed using levelized cost of energy (LCOE) in other instances, the analysis was restricted to a project cost without the application of LCOE metrics.

Multi-criteria Assessment

The selection of optimal configurations considered technical performance (thermal power output, temperature stability, system efficiency), economic viability (payback periods, LCOE comparison with alternatives), and integration feasibility (compatibility with existing infrastructure, operational flexibility). Sensitivity analyses were performed on key parameters including energy prices, carbon costs, and subsidy levels to assess economic robustness under varying market conditions.

This project has received funding from the European Union's Horizon Europe research and innovation program under grant agreement No 101083558

3. Results

3.1. French case study

3.1.1. Introduction

Historically, district heating networks in France have been used to serve relatively dense groups of buildings requiring large amounts of energy. The engineering of most existing networks is designed for this type of demand: sources capable of providing large quantities of heat and distribution at 'high temperature' (supply at 100°C, return at 70°C). With the development of low-energy neighbourhoods, the thermal renovation of existing buildings, and the rise of low-temperature emitters (e.g., underfloor heating), heat demands in a given area may be lower. In this case, a low-temperature network (supply at 70°C, return at 35°C) is more suitable.

3.1.2. District heating network

The site of Fresnes, south of Paris, near Paris Orly airport, has been selected as one of the case studies for considering the HOCLOOP concept. There, a geothermal plant is already in operation producing hot water from the Dogger reservoir, and it is connected to the district heating system. At the present day, the primary fluid is produced from the GFR-3 well at 73°C with a 250 m^3/h (around 70 kg/s) flowrate. The produced fluid goes through the filtration, the heat exchangers, before being reinjected between 41 and 35°C in wells. If the outside temperatures fall below 8°C, a thermal heat pump is used after the heat exchangers and the temperature of the reinjected brine is falling to 25°C. Thus, a total thermal energy of around 9-14 MW, depending on the reinjection temperature, is produced. For an outside temperature below 6°C, a parallel cogeneration turbine is used. Emergency turbines are also present for maintenance or any breakdown of the installations. In 2016 the geothermal power plant (with the heat pump) produced around 51 GWh and 40 GWh additional were delivered by other sources (cogeneration and gas turbines). The existing network covers around13 km of pipes, with 104 delivery points and 90 sub-stations.

3.1.3. Integration of the HOCLOOP concept

In the deliverable 4.2, the potential of deploying the HOCLOOP concept by repurposing the injection well GFR-3 was investigated. Using a well flow simulator (GWellFM) several simulations were performed, and it was shown that it would be necessary to extend vertically the well for 500 m before considering a horizontal extension of 2 km. Due to the highly transient nature of the heat conduction transfer from the rocks to the wellbore, the outlet temperature of the fluid decreased by several degrees, with the phenomenon being more important during the first stages of the operation. For the system to be able to deliver to the district heating system a fluid with constant temperature, the inlet conditions must be controlled. From the two optimization procedures tested (D4.2), adjusting the inlet flow rate proved to be the optimal method in comparison with the control of the inlet temperature. In overall, even with a potential horizontal extension of the wellbore, the produced power from one closed system was four (around 0.01 MW) to three (0.1 MW) orders of magnitude lower than the actual production of the geothermal doublet (10 MW).

3.1.4. Coupled simulations

3.1.4.1. Surface model modelling

The well model (GWellFM) described in deliverables D2.1-2.5 [5, 6, 7, 8, 9] is now coupled with a surface

This project has received funding from the European Union's Horizon Europe research and innovation program under grant agreement No 101083558

model to estimate the net energy production. The surface installation includes a system of heat exchange, a pump and the necessary piping to connect the system with the wellhead.

The replication and modelling of the equipment of the surface installation is made in COCO, the CAPE-OPEN to CAPE-OPEN steady-state simulation environment. The properties calculated by the different equipment are obtained with Python Unit Operation (PUO). PUO is a CAPE-OPEN based unit operation, for which the calculations are performed with a Python script. Python scripts are designed to perform detailed thermodynamic calculations, using input conditions of the fluid and a set of parameters to determine the output fluid properties and calculated parameters of the unit.

For flowsheet modelling, COFE v3.8.0.1 (the CAPE-OPEN Flowsheet Environment) is used. COCO/COFE is a steady-state free-of-charge sequential chemical flowsheet simulator with an intuitive graphical user interface.

3.1.4.1.1. Heat exchanger

The modelling of heat exchange is conducted through a comprehensive thermodynamic model of a plate heat exchanger operating in counter-current configuration. This configuration maximizes the temperature difference between fluids throughout the heat exchanger, optimizing thermal effectiveness compared to co-current flow arrangements and allowing for closer approach temperatures.

The heat exchanger model incorporates four material ports defining the fluid flow paths through the system. Feed 1 and Product 1 represent the hot fluid inlet and outlet respectively, handling the geothermal fluid where water circulates in a closed loop and heats up as it circulates in the well. Feed 2 and Product 2 constitute the cold fluid inlet and outlet for water from a low-temperature urban heating network as illustrated in Figure 1.

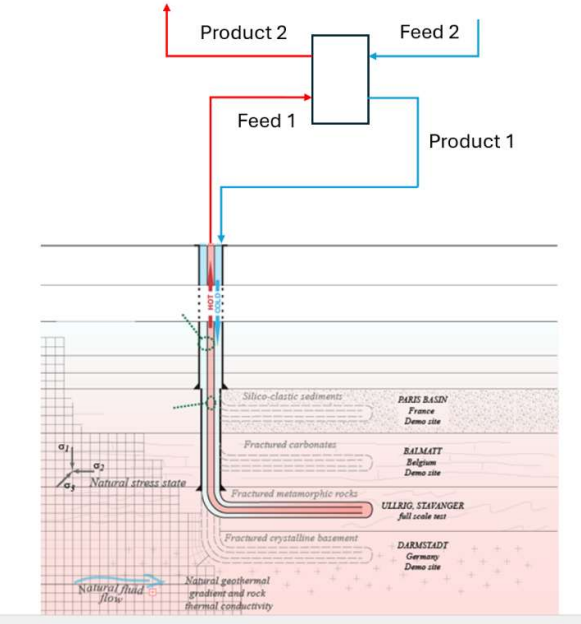

Figure 1. Heat exchanger integration.

The model requires thermodynamic parameters including target temperatures for the cold fluid to establish desired thermal performance objectives, while Product 1 temperature is determined through HOCI criteria

This project has received funding from the European Union's Horizon Europe research and innovation program under grant agreement No 101083558

design of 5°C. Geometric parameters play a crucial role in determining performance characteristics. The plate length and width define the primary heat transfer surface dimensions directly influencing available area for thermal exchange. The channel gap specifies spacing between adjacent plates, affecting both heat transfer coefficients and pressure drop characteristics. The port diameter determines inlet and outlet connection sizes, impacting fluid distribution and pressure losses at manifolds. The chevron angle represents the corrugated pattern angle on plates, significantly influencing heat transfer enhancement and pressure drop penalties. The surface enlargement factor accounts for increased effective surface area due to plate corrugations compared to smooth plates. The number of passes defines how many times fluid traverses the heat exchanger, affecting both thermal performance and pressure drop. Material properties are captured through plate thickness and conductivity parameters, determining conductive resistance through the plate material. Table 1 details the different values given to these parameters.

Table 1. Characteristics of the plate heat exchanger (Paris case) [10, 11].

Parameter	Value
Plate length (m)	1.55
Plate width (m)	0.8
Channel gap (mm)	5
Port diameter (m)	0.2
Plate thickness (mm)	0.6
Plate conductivity (W/m/K)	17.5
Chevor angle (°)	45
Number of passes	1
Surface enlargement factor	1.25

The model generates comprehensive output data encompassing thermal, hydraulic, and sizing parameters. The required heat transfer represents total thermal power that must be exchanged to achieve specified temperature targets, serving as the fundamental design criterion. The calculated cold fluid flow rate is determined through energy balance calculations, ensuring the cold fluid can absorb required thermal energy while reaching its target temperature. The overall heat transfer coefficient U represents overall thermal conductance per unit area, while the heat exchanger surface area quantifies the total effective area required for heat transfer.

Calculation of overall heat transfer coefficients involves determining convective heat transfer characteristics for both fluid streams using hydraulic diameter concepts [12, 13, 11]. The equivalent diameter is calculated as twice the channel height, with hydraulic diameter adjusted for the surface enlargement factor. Mass velocity calculations for both channel flow and port flow provide the basis for Reynolds number determination, which characterizes the flow regime. The Reynolds number, combined with the Prandtl number, enables application of modified Dittus-Boelter correlations for calculating individual heat transfer coefficients. The overall heat transfer coefficient combines individual convective resistances with conductive resistance through the plate material, accounting for all thermal resistances in the heat transfer path.

This project has received funding from the European Union's Horizon Europe research and innovation program under grant agreement No 101083558

Pressure drop calculations incorporate multiple pressure loss mechanisms including friction losses in flow channels, form losses at inlet and outlet ports, and gravitational pressure differences [12]. The friction factor correlation accounts for chevron angle effects on flow resistance, with mathematical relationships incorporating both Reynolds number dependence and geometric effects specifically developed for corrugated plate geometries [10].

Sizing calculations determine physical dimensions required to achieve specified thermal performance. The effective surface area of each plate accounts for both sides and includes the surface enhancement factor due to corrugations, with a corrugation factor of 1.2 being typical for commercial plate heat exchangers with standard chevron patterns. The number of plates required is determined by dividing total required heat transfer area by effective area per plate, ensuring the final configuration meets thermal requirements while providing realistic estimates of physical dimensions.

The heat exchanger design process is illustrated through the flowchart shown below in Figure 2.

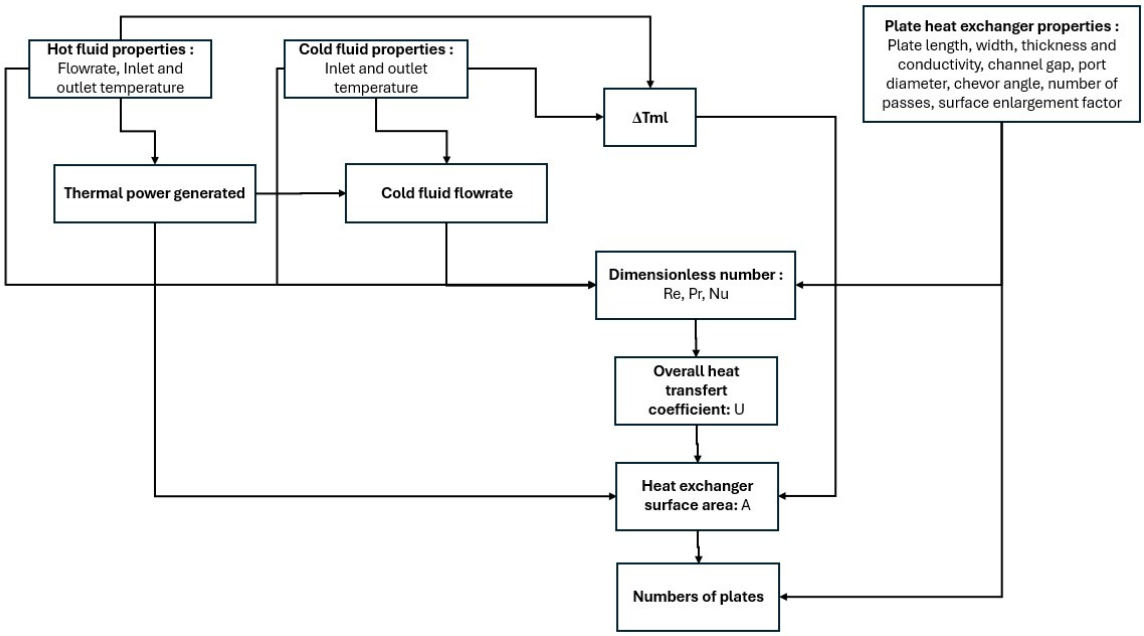

Figure 2. Flowchart of the design process for the plate heat exchanger.

A second heat exchanger model has been developed to address different design constraints and operational requirements. This alternative model operates according to the same fundamental thermodynamic principles and utilizes identical correlations for heat transfer and pressure drop calculations as the primary model. The counter-current flow configuration is maintained to preserve optimal thermal effectiveness, and the same four material ports define the fluid flow paths through the system.

The key distinction of this second model lies in its design approach: rather than calculating the required heat exchanger surface area based on specified thermal performance targets, the heat exchanger surface area is predetermined and fixed as an input parameter.

With the surface area constraint established, the model employs an iterative calculation methodology to determine the optimal flow rates for cold fluid circuit whereas flow rate for hot circuit remains constant. The calculation process involves solving the coupled energy and momentum balance equations

This project has received funding from the European Union's Horizon Europe research and innovation program under grant agreement No 101083558

simultaneously to achieve the desired outlet temperature for cold fluid stream. The hot fluid outlet temperature (Product 1) is determined by the enthalpy balance across the heat exchanger, which is intrinsically linked to the fixed surface area of the exchanger.

3.1.4.1.2. Pump

The pump model establishes two ports representing the fluid inlet and outlet, maintaining mass conservation while tracking thermodynamic state changes. The model incorporates isentropic efficiency to account for real-world irreversibilities, distinguishing it from idealized thermodynamic calculations.

The input parameters are of the outlet pressure and isentropic efficiency, which completely define the operating conditions and performance characteristics. These parameters enable the model to calculate work required by the pump.

The calculation begins by extracting inlet properties including enthalpy H1, entropy S1, pressure P1, temperature T1, and mass flow rate from the feed stream. These properties establish the initial thermodynamic state that serves as the reference point for subsequent calculations.

The core thermodynamic analysis determines the isentropic end state. This approach solves the entropy constraint equation S2 = S1 at the specified outlet pressure P2. Corresponding ideal outlet temperature T2 and ideal enthalpy H2 are computed. Once the isentropic end state is determined, the model applies the isentropic efficiency correction to calculate real outlet properties enthalpy H2_real, entropy S2_real, pressure T2_real. The total work transfer is then calculated by multiplying the real enthalpy change by the mass flow rate.

Considering eventual thermo-siphon effect of the fluid within the well. The model automatically distinguishes if the use of the pump can by bypass. When P2 > P1, the system operates as a valve, performing an isenthalpic expansion process without any energy generation. In this valve configuration, the working fluid undergoes pressure reduction at constant enthalpy, dissipating excess pressure through irreversible throttling losses.

Under these conditions, the injection pressure remains constant and equal to 10 bar, ensuring consistent system operation regardless of the upstream pressure variations and maintaining optimal fluid injection characteristics for the geothermal system.

3.1.4.1.3. Tubing

The model also provides a comprehensive pressure drop calculation for surface piping installation, employing the Churchill correlation to determine accurate friction factors across all flow regimes. The model requires three fundamental input parameters: pipe total length (m), pipe diameter (m), and surface roughness (m), which collectively define the geometric and surface characteristics of the flow system. Consequently, the model calculates the pressure drop (Pa) in the surface pipes both upstream and downstream of the heat exchanger. The pipeline configuration assumes 100 m of piping to connect the well to the heat exchanger and an additional 100 m to return from the heat exchanger to the well.

3.1.4.2. Results

The coupled simulations were run with the first model of heat exchanger for a period of 10 years in order to estimate the necessary surface of the heat exchanger. As shown in Deliverable 4.2, for a constant flow rate the well outlet temperature decreases with time due to the transient nature of the heat transfer mechanism. The results demonstrate that the well outlet temperature is significantly higher during the

This project has received funding from the European Union's Horizon Europe research and innovation program under grant agreement No 101083558

initial phases of exploitation. The data clearly indicate an inverse relationship between mass flow rate and outlet temperature: lower flow rates yield higher outlet temperatures due to increased residence time within the geothermal reservoir, allowing for more complete heat transfer between the rock formation and the circulating fluid.

However, a contradiction is observed in the temperature profiles during the initial time steps, where this expected relationship is not maintained. This anomaly is attributed to initialization issues within the numerical model, where the initial conditions may not accurately represent the fully developed thermal and hydraulic state of the system. These transient effects are characteristic of the model's convergence behavior during the early computational stages.

The analysis reveals a critical operational threshold: well exploitation must be terminated when the outlet temperature drops below 70°C. This temperature limit is imposed by the thermal cross-over phenomenon with the secondary fluid circuit, which operates at an outlet temperature of precisely 70°C. Below this threshold, the temperature difference becomes insufficient to maintain effective heat transfer across the heat exchanger, rendering the geothermal system thermodynamically inefficient and economically unviable.

The thermal power recovery profiles demonstrate a direct correlation with the previously observed outlet temperature trends. Higher mass flow rates initially yield greater thermal power output. However, the thermal power exhibits a continuous decline over the exploitation period due to reservoir thermal depletion.

The relationship between flow rate and sustained thermal power recovery reveals an optimal balance: while higher flow rates provide greater initial power output, they also accelerate reservoir cooling, leading to steeper decline curves. Conversely, lower flow rates maintain more stable thermal production over extended periods. This behavior directly correlates with the outlet temperature analysis, where lower flow rates preserved higher temperatures due to enhanced heat transfer efficiency within the reservoir.

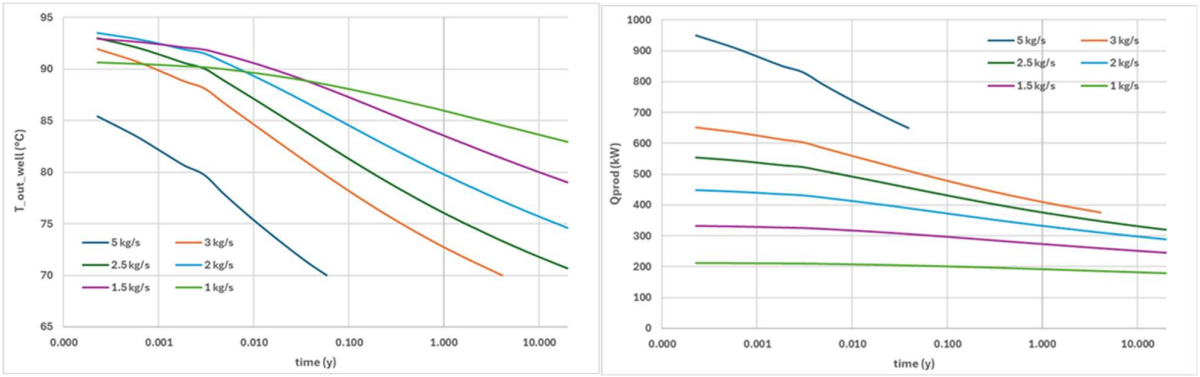

Figure 3. Evolution of outlet geothermal fluid temperature (left) and thermal power recovery (right) for non-constant heat exchanger surface area (Paris case).

The surface area requirements demonstrate an exponential relationship with operational time, with higher flow rates necessitating significantly larger heat exchanger surfaces as reservoir temperatures decline. This behavior reflects the fundamental heat transfer principle where reduced temperature differentials require proportionally increased surface areas.

Based on this analysis, the selected operational flow rate is 2 kg/s, which corresponds to a well outlet temperature of 75°C at the end of the exploitation period. Given that the secondary loop operates at a production temperature of 70°C, this 5°C temperature difference represents an economic optimum that

This project has received funding from the European Union's Horizon Europe research and innovation program under grant agreement No 101083558

provides a compromise between thermal power recovery and heat exchanger sizing requirements.

This temperature differential is critical for economic viability, as demonstrated by the surface area trends shown in the figure, where heat transfer surfaces tend toward infinity when the temperature difference becomes too small. The 2 kg/s flow rate therefore balances maximum energy extraction with practical heat exchanger dimensions, avoiding the prohibitive costs associated with oversized equipment that would be required for smaller temperature approaches while ensuring sufficient thermal driving force for efficient heat transfer throughout the system's operational lifetime.

The discontinuous behavior observed in the heat exchanger surface area curves is attributed to the discrete nature of the plate heat exchanger design, where the required number of plates must be an integer value, creating step-wise increases in surface area as thermal performance demands exceed the capacity of the current plate configuration, combined with numerical convergence artifacts inherent to the coupled iterative algorithm solving simultaneously for pressure drops, heat transfer coefficients, and geometric constraints.

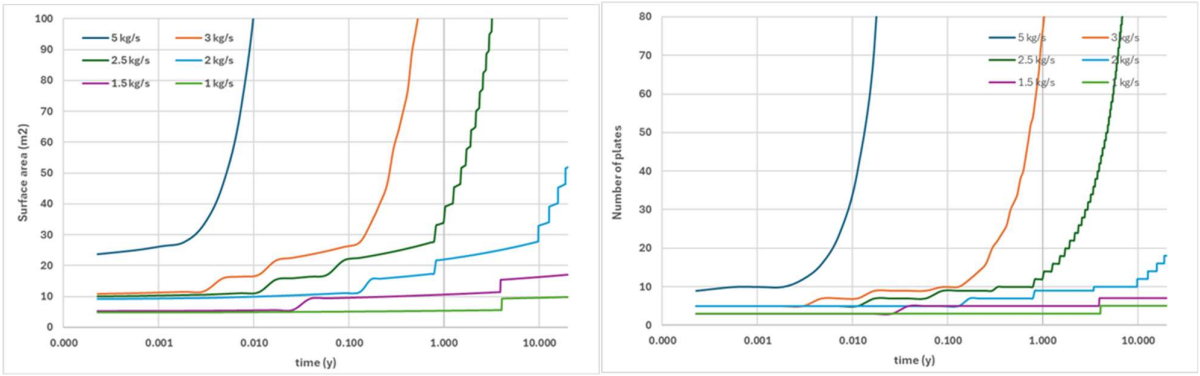

Figure 4. Evolution of the heat exchanger surface (left) and number of plates (right) with non-constant heat exchanger surface area (Paris case).

The analysis reveals that at lower flow rates, the well outlet pressure exceeds the injection pressure (10 bar) due to the thermosiphon effect, where natural circulation is generated by the density differential between the heated ascending fluid and the cooler descending fluid. Over time, this outlet pressure exhibits a gradual decline, which correlates directly with the decreasing outlet temperatures that reduce the fluid density differential and consequently diminish the thermosiphon driving force.

Conversely, at higher flow rates, the friction losses generated within the wellbore exceed the pressure recovery from the thermosiphon effect, resulting in well outlet pressures that fall below the injection pressure threshold. Under these operating conditions, the natural thermosiphon mechanism becomes insufficient to overcome the hydraulic resistance, necessitating the implementation of a mechanical pumping system to compensate for the net pressure losses and maintain adequate circulation within the geothermal loop. In our case study, mechanical pumping is only required above a flow rate of 3 kg/s, as illustrated in Figure 5. Regarding the surface pressure losses, which were calculated for both the piping network and the heat exchanger, these remain low due to the relatively low flow rates employed in the system. Table 2 details these surface pressure losses as a function of flow rate.

This project has received funding from the European Union's Horizon Europe research and innovation program under grant agreement No 101083558

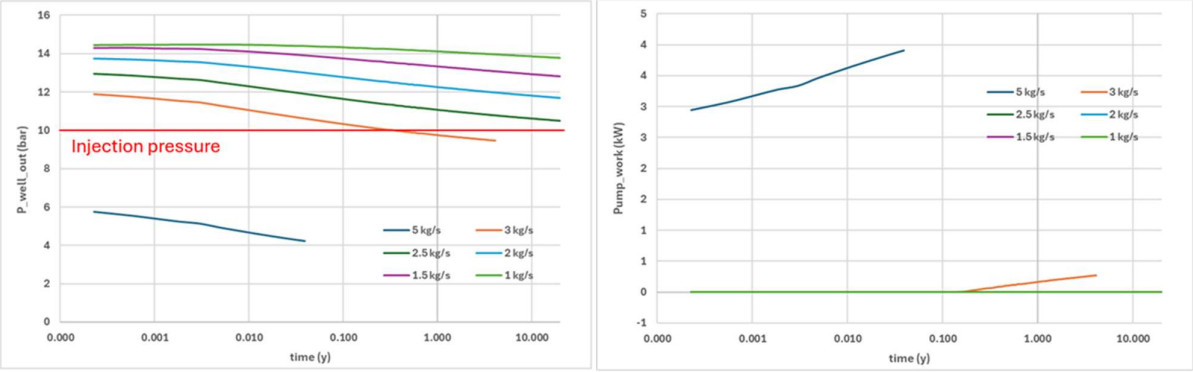

Figure 5. Evolution of outlet geothermal fluid pressure (left) and power consumption of the pump (right) with non-constant heat exchanger surface area (Paris case).

Table 2. Surface equipment for different flowrate (Paris case).

Flowrate (kg/s)	1	1.5	2	2.5	3	5
Total pressure drop (bar)	0.083	0.101	0.128	0.164	0.206	0.439

A parametric study was conducted using the second heat exchanger model, where the heat transfer surface area and flow rate are specified as fixed input parameters. The analysis examined heat exchanger surface areas ranging from 25 to 45 m² at a constant flow rate of 2 kg/s to determine the corresponding outlet temperatures and thermal energy generation for each configuration.

The parametric analysis reveals that heat exchanger surface area variations between 25 and 45 m² produce negligible differences in both outlet temperature and thermal power recovery profiles. This convergence behavior indicates that the system performance is not limited by heat transfer area within this range, but rather by other controlling factors.

The outlet temperature profiles, and the thermal power curves show remarkably similar trajectories across all surface area configurations. This suggests that the reservoir thermal depletion is the dominant mechanism governing temperature and thermal power decline, rather than heat exchanger limitations.

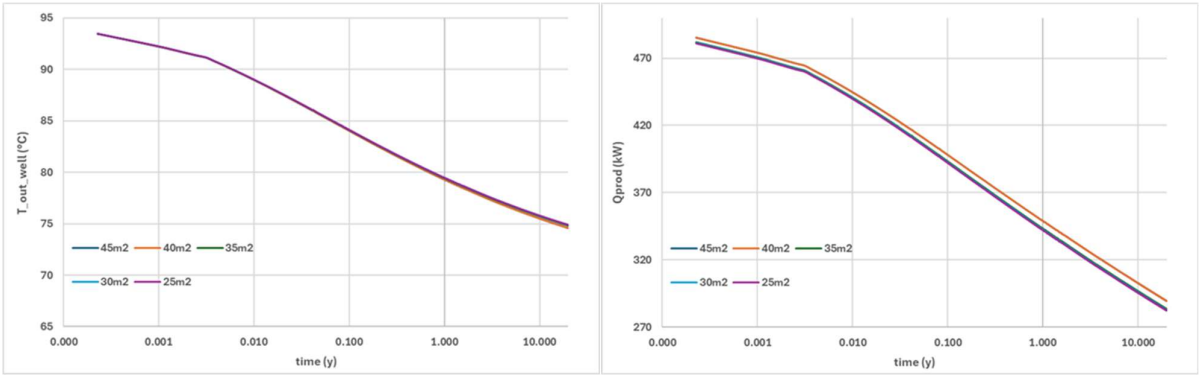

Figure 6. Evolution of outlet geothermal fluid temperature (left) and thermal power recovery (right) for different fixed heat exchanger surface area and for a 2kg/s fluid circulation (Paris case).

By integrating the recovered thermal power over the respective time intervals, the total energy extracted throughout the well's operational lifetime can be determined for each configuration. Subsequently, the average thermal power extraction rate can be calculated by dividing the cumulative energy by the

This project has received funding from the European Union's Horizon Europe research and innovation program under grant agreement No 101083558

exploitation duration. The results are presented in the following Table 3.

Table 3. Energy performance summary for variable heat exchanger surface areas (Paris case).

Heat exchanger surface	25 m²	30 m²	35 m²	40 m²	45 m²
Total energy extracted (GWh)	27.63	27.69	27.76	28.25	28.26
Average thermal power extraction rate (kW)	315.4	316.1	316.9	322.5	322.6

As detailed, under the optimal operating conditions determined above, the circulation flow rate was fixed at 2 kg/s. The results indicate that the thermosiphon effect provides sufficient driving force to eliminate the requirement for mechanical pumping. However, for practical operational considerations, particularly during system startup procedures, a circulation pump is incorporated into the process and instrumentation diagram (P&ID) and included within the scope of the techno-economic evaluation. Technical information about pump design is detailed in Table 4.

Table 4. Pump technical information.

Type	Centrifugal pump
Flow	7.26 m^3/hr
Shaft power brake	4.8 kW

3.1.4.3. PID Diagram

A P&ID (Piping and Instrumentation Diagram) of the surface installations for a geothermal heat recovery site has been developed and is available in the Appendix. This diagram specifies the various instrumentation around two key equipment pieces: the plate heat exchanger and the pump. The detailed description of the different instrumentation is provided in the accompanying technical documentation.

The instrumentation around the Plate Heat Exchanger includes:

- Temperature sensors at the inlet and outlet of each circuit (hot and cold) to measure inlet/outlet temperatures. These measurements enable thermal transfer calculations and control regulation.
- Flow meters are installed on each supply line to measure fluid flow rates, positioned upstream of the exchanger on both hot and cold circuits.
- Pressure gauges are mounted at the inlet and outlet of each circuit to calculate differential pressure across the exchanger. Abnormally high-pressure differentials indicate fouling or obstruction of the plates.
- Isolation valves are positioned upstream and downstream of the exchanger on each circuit to isolate the equipment during maintenance or interventions. In addition, connections for eventual cleaning are installed with drains. Safety valves are installed at both outlets of the heat exchanger in case of thermal expansion of the fluids.

The instrumentation around the pump includes:

- Flow meters positioned at the pump outlet to monitor actual flow rates.
- Pressure sensors are installed on the suction side to monitor suction pressure and ensure available NPSH, and on the discharge side to control pump operation, prevent cavitation, and detect blockages or wear. Also, the pressure sensor installed at the suction side of the pump controls the pump injection pressure. If the upstream pressure is higher than the pump setpoint, which is

This project has received funding from the European Union's Horizon Europe research and innovation program under grant agreement No 101083558

possible if the thermosiphon effect in the well is significant, the bypass is activated, and the PV011 valve regulate the injection pressure at 10 bar. At the same time the pump is stopped.

- Additional safety equipment includes isolation valves, and check valve.

3.1.5. Cost analysis

The cost estimation begins with the calculation of the cost of equipment and utilities. These estimates are based on the size of the equipment and utility consumption determined in the part 3.1.4.2. In our case, we need to calculate the cost of a pump and a plate heat exchanger. The cost estimation of equipment will be carried out by Estime an internal tool developed by IFPEN. The Estime software is based on the PRE-ESTIME [14] and is used to estimate the costs of numerous pieces of equipment, including their installation, surroundings and instrumentation, such as pumps, compressors, reactors, heat exchangers.

For utility consumption, electricity could be considered. But, in the present case study, it has been demonstrated that the thermosiphon effect provides sufficient driving force for fluid circulation without requiring mechanical pumping. Consequently, no utility consumption is considered.

Also, a cost of drilling is considered, the below figure gives a short description of the well design and subsurface lithology. The case to be considered is an extension of 500 m of the existing well deeper in the reservoir and then 2 km of horizontal extension, i.e. a total well deepening of 2.5 km. Since the lower open hole formation is permeable, it is judged required to install a 7" liner in the lower section of the well before installing the completion tubing.

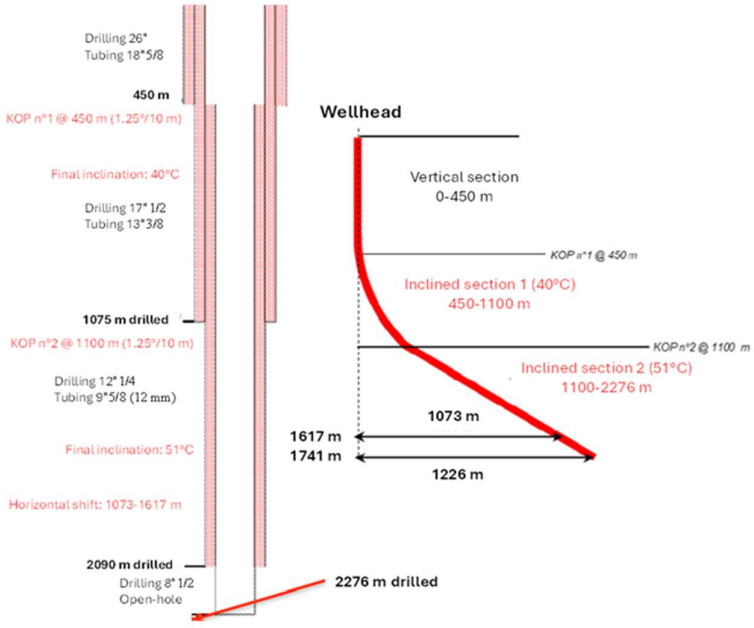

Figure 7. Desing of the GFR-3 geothermal wellbore in the French site.

Table 6 gives some key data for the well and Table 7 gives a summary of the cost estimate for the operation to install a suitable DHS for the well. The well is assumed to have easy access for the well intervention. The cost for the removal of any existing completion string in the well prior to the operation is not included in the cost estimates presented here. Neither is the costs associated with the connection of the well to the surface heat system. The operation is judged possible using a medium size drilling rig. No special drilling issues are reported. The cost estimate covers the well deepening of the 8 ½" section, 7" liner installation in

This project has received funding from the European Union's Horizon Europe research and innovation program under grant agreement No 101083558

the open hole section and installation of the DHS with 4.5" OD.

Table 5. Thermal properties of all geological layers for the Paris basin.

Layer	Bottom [m MD]	Temperature [°C]	Conductivity [W/m²/°C]	Capacity [J/°C/kg]	Density [kg/m³]
Surface	0	15	-	-	-
Albian	548	30.6	1.59	903	2380
Gault shale	608	32.6	3.16	859	2270
Barremian	754	38.3	1.63	915	2480
Oxfordian	1322	58.4	2.24	795	2390
Callovian	1623	68.1	1.73	917	2590
Lower Callovian	1727	71.7	2.14	805	2450
Bathonian	1767	73.7	2.14	806	2590
Dommerian	1963	81.0	1.74	915	2600
Rhetian	2146	88.0	2.63	887	2510
Anisian	2590	100.4	2.94	710	2370

Table 6. Well data for the French case.

Parameter	Before deepening	After deepening
Measured Depth	2.3 km	4.8 km
True Vertical Depth	1.7 km	2.0 km
Operation concerns	-	

Table 7. Drilling cost estimates for the French case.

Cost item	Time	[M€]
Mob/Demob and site preparation	1 week	1
Well operation (24/7)	3 weeks	2
Equipment, tubulars and consumables	-	4
Sum		7

The financial analysis allows the determination of the cost of heat after calculating the costs of equipment, utilities and drilling, in the context of a precise financial environment. The analysis was carried out using the tool developed by IFPEN "CalDev". It is a spreadsheet can that allows to calculate the CAPEX and OPEX of the project and the Net Present Value for the different cases. The economic parameters for this project are displayed in Table 8.

Outside battery limits (OSBL) costs represent the project costs outside the battery limits. It includes infrastructure, engineering costs and contingencies. For this project, OSBL costs represent a percentage of ISBL (Inside Battery Limits) costs, and are specified in Table 9.

Table 8. Value of economic parameters for the financial analysis.

Economic parameter	Value	Economic parameter	Value

This project has received funding from the European Union's Horizon Europe research and innovation program under grant agreement No 101083558

Construction period (yr)	1	Cost of debt (%)	6
Project lifetime (yr)	20	Loan tenure (yr)	10
Depreciation (yr)	10	Debt (%)	30
Residual value (%)	10	Equity (%)	70
Tax rate (%)	30	Cost of equity (%)	15
Inflation rate (%)	2	Discount rate (%)	8

Table 9. OSBL costs as a fraction of ISBL costs.

OSBL cost	% ISBL
Infrastructure	5 %
Engineering	10 %
Contingencies	15 %

Direct and indirect installed costs make up the total installed costs (CAPEX). Direct costs are taken as 5% of the ISBL for the spare parts. Indirect costs (licensing, training, legal, start-up) represent 10% of the ISBL costs. Labor costs and fixed charges (maintenance, insurance and overheads) constitute fixed costs (OPEX). Labor costs are considered to be 1% of the ISBL costs. Maintenance, insurance and overhead represent 1.5%, 0.5% and 1% of the ISBL costs, respectively. The cost estimations of the equipment and cost of energy is detail in the following Table 10, it summarizes the various thermal power recovery scenarios for different heat exchanger surface areas:

Table 10. Cost estimation of erected equipment & cost of energy for different heat exchanger surface.

Heat exchanger surface scenario	25 m²	30 m²	35 m²	40 m²	45 m²
Average thermal power extraction rate (kW)	301.7	302.4	303.2	308.9	308.9
Cost of erected heat exchanger (k€)	164	168	172	177	180
Cost of erected pump (k€)	126	126	126	126	126
Design process allowance cost (k€)	29	30	30	31	31
ISBL cost (k€)	319	324	328	333	337
Cost of energy (€/kWh)	0.3869	0.3864	0.3858	**0.3789**	0.3793

3.1.6. Discussion

For the French case study, the optimal energy cost is achieved with a heat exchanger surface area of 40 m² and a geothermal fluid circulation rate of 2 kg/s, yielding an energy cost of 0.3789 €/kWh. This cost remains significantly elevated compared to conventional energy sources, which typically range from 0.05-0.15 €/kWh. This economic disadvantage stems from the limited energy recovery relative to the substantial capital investment required for well installation and equipment. The well drilling and installation costs amount to 7,000 k€, while equipment costs total 333 k€, resulting in a well-to-equipment cost ratio of approximately 21:1. This disproportionate capital structure highlights that the primary economic constraint lies in the high upfront investment for well development rather than surface equipment costs.

This project has received funding from the European Union's Horizon Europe research and innovation program under grant agreement No 101083558

The project lifetime consideration deserves particular attention in the economic analysis presented. While the initial energy cost calculation of 0.3789 €/kWh assumes a 20-year amortization period, this assumption warrants re-examination given the specific characteristics of closed-loop geothermal installations. These systems inherently benefit from exceptionally long operational lifespans with minimal degradation over time, which justifies exploring different temporal horizons for the economic assessment.

Sensitivity analysis across various project lifetimes reveals a significant decrease in energy costs as the amortization period extends. (Table 11)

Table 11. Cost of energy for different project lifetime (French case)

Project lifetime considered (yr)	10	20 (ref)	30	50
Cost of energy (€/kWh)	0.565	0.379	0.329	0.293

However, this temporal analysis raises critical questions about the consistency of component lifetime assumptions. The presumption of a 50-year lifespan for surface equipment, including pumps, heat exchangers, and control systems, appears optimistic when compared to the inherent robustness of a geothermal well. In practice, properly constructed wells can operate well beyond 50 years with minimal maintenance, whereas mechanical surface equipment typically requires replacement or major renovation after 20-30 years of operation. This asymmetry in component durability suggests that the economic model may overestimate the longevity of certain system elements.

The extension of techno-economic analysis to a 50-year horizon also raises legitimate concerns about analytical relevance. Industrial practice rarely extends feasibility studies beyond 30 years for compelling reasons. Beyond this timeframe, predictions regarding energy prices, maintenance costs, and technological evolution become highly speculative. Furthermore, the economic impact of financial flows beyond 30 years becomes marginal when applying typical discount rates of 5-10%, and technological advances may render the installation less competitive well before the end of its physical life. Most investors and financial institutions consequently limit their analyses to a maximum of 25-30 years, reflecting established industry standards for long-term infrastructure investments.

3.2. Belgium case study

3.2.1. Introduction

Two options were proposed for the Balmatt case study in D4.1 and investigated numerically in D4.2. The first would utilize the existing well MOL-GT-03 to preheat the working fluid of the heating network, thus reducing the demand on the deep geothermal doublet and gas at the boiler house. This approach would also result in a slightly warmer injection temperature. The relatively return temperature (60 °C) would result in less efficient use of MOL-GT-03 due to heat losses in the shallower depths. The well would supply a thermal power between 250-300 kW if used in that case. The second scenario investigated was the possible use of the well to provide the heating for new office buildings Earth A and Earth B being planned at VITO. In that scenario, the injection temperature would be around 40 °C and the numerical study showed the well could entirely provide the heating demand of the new building for more than 20 years. This would result in a more efficient use of the well's heat. The predicted demand was seasonal, but the well could provide an average thermal power like the first scenario but could also deliver 12-hourly peaks greater than 600 kW.

The second scenario of heating Earth buildings A and B was the preferred option at VITO since that was

This project has received funding from the European Union's Horizon Europe research and innovation program under grant agreement No 101083558

more efficient manner to use the heat and required no further drilling. For this design and techno-economic analysis, we consider only the second scenario of heating the newly planned VITO office buildings.

3.2.2. District heating network

For the Belgian case study, the focus is the integration of the HOCLOOP concept in the 3rd well of the Balmatt site and to use the heat for building heating of new office and lab building of VITO (the Earth building, existing of two separate buildings, namely Earth building A and Earth building B).

Currently, the third well at Balmatt (MOL-GT-03) is used for research and monitoring purposes and is not in operation. The well has been equipped with a liner and completion string. More detailed description can be found in HOCLOOP D4.1.

The current concept for heating and cooling the new Earth buildings is an ATES system combined with a heat pump and chillers. For this case study an analysis is made to deliver the heating via the HOCLOOP concept. In order to transport the heating from the 3rd well of Balmatt to the Earth building A and B a district heating network is needed.

In further analysis, two cases for the district heating network were analyzed. The first case was a district heating network above ground and the second case was a district heating network below ground.

To physically separate the building heating circuit with the circuit of the HOCLOOP concept and the district heating network, a heat exchanger is included in both Earth building A and Earth building B. There is no heat exchanger between the HOCLOOP concept, and the district heating network included in order to avoid higher capex and reduction of the temperature level in the district heating network.

The proposed network trace is shown in Figure 8. The third well of Balmatt is located at the bottom of the map. The proposed network trace is marked in orange and has a length of about 834 m to both Earth buildings.

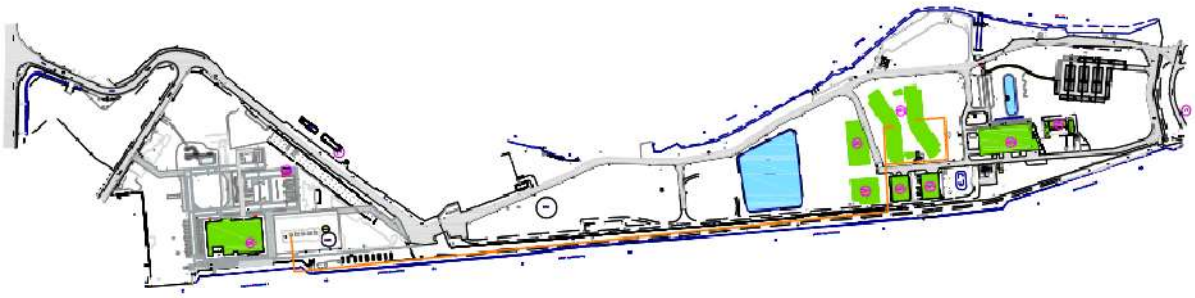

Figure 8. Proposed network trace from the 3rd well of the Balmatt site to the Earth buildings (network trace is marked in orange).

3.2.3. Integration of the HOCLOOP concept

To integrate the HOCLOOP concept to provide the heat demand for the new VITO buildings would require additional infrastructure on the surface. The buildings are some distance (~1 km) from the MOL-GT-03 location, so some distance of insulated piping is required. The cooling requirement of the buildings would have to be provided by another source. In the further analysis, we do not take into account the cooling demand, but as a potential source for cooling an air-water heat pump with heat recuperation would have been chosen. This means that the cooling and heating systems would require separate piping systems to

This project has received funding from the European Union's Horizon Europe research and innovation program under grant agreement No 101083558

connect to the new office buildings. The heating system would also require a heat exchanger in each building (A and B) to transfer the heat from the well to the buildings.

3.2.4. Simulation approach

The subsurface simulation approach was detailed in Task 4.2. An estimated demand profile for both 12-hourly demands and monthly average demands was created by VITO, then used to simulate the subsurface behavior and subsequent heat delivery from the existing MOL-GT-03 for 20 years using the IFE-developed tool GTW. The flowrate, pressure drop, and delivery temperature were all simulated to deliver exactly the demanded thermal power over time. The results of thermal heat delivery and outflow temperature can be seen in Figure 9. A coupling with a heat network/heat exchanger simulator was not carried out, but rather, a system (below) was proposed that could handle the required temperatures, pressures, and flowrates for supplying the delivered heat to the newly planned VITO buildings A and B.

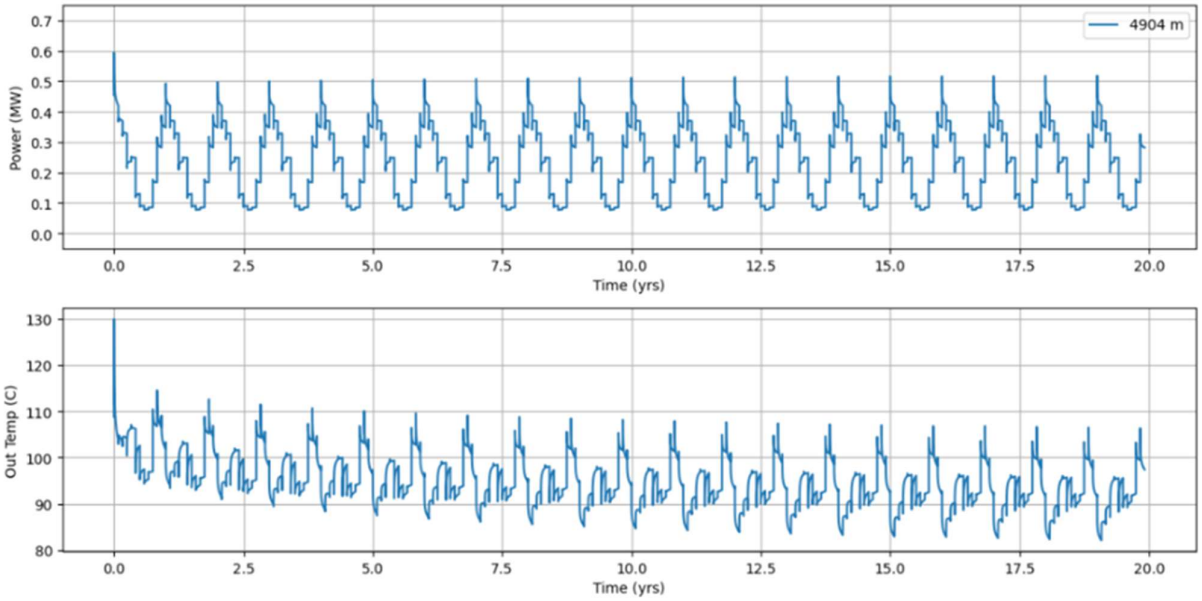

Figure 9. Simulated thermal power and outflow temperature of MOL-GT-03 if completed with the HOCLOOP concept.

3.2.5. Cost analysis

3.2.5.1. HOCLOOP system

The well has a lateral deviation of more than 2 km shown in Figure 10. The length of the well is 4,950 meters and the True Vertical depth (TVD) is 4,234 meters. More details of the well can be found in HOCLOOP D4.1 [1].

The well has easy access, however, the well already has an existing completion string installed. The string needs to be removed prior to the operation. The cost for the removal of the existing completion string is not included in the cost estimates presented here. Since there currently is negligible leakage rates when pressurizing the well, it is assumed that the well can be used for closed loop circulation without a liner installed in the lower well section.

Due to the restriction in the well at 3,533 m depth, the use of a DHS with 4.5" OD will allow to pass the restriction and reach the bottom of the well. This DHS size is considered suitable for this case, because of the predicted low circulation rates for the heat extraction from the well.

This project has received funding from the European Union's Horizon Europe research and innovation program under grant agreement No 101083558

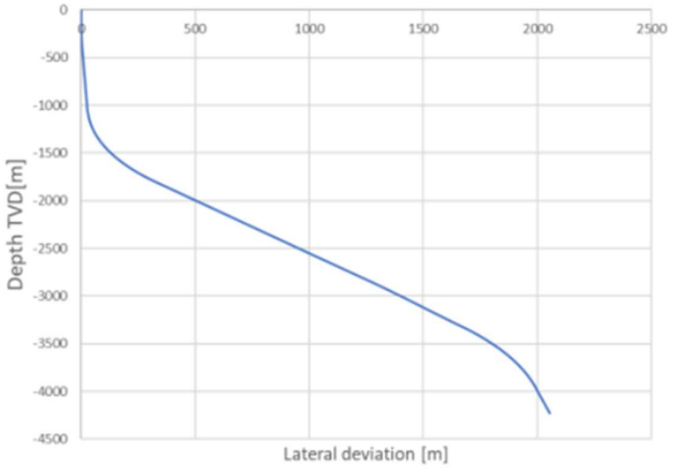

Figure 10. Well trajectory of MOL-GT-03.

The operation to install the DHS is considered possible by using a rig-less intervention unit and heavy-duty cranes. This is a low-cost alternative to the commonly used workover rigs for such operations. Table 11 gives an overview of the cost of the installation of the HOCLOOP concept in the 3rd well of Balmatt. The total cost is estimated to be 2.3 M€.

Table 11. Cost estimates to install HOCLOOP system in existing well MOL-GT-03.

Cost item	Time	[M€]
Mob/Demob and site preparation	1 week	0.1
Well operation (daytime)	4 weeks	0.6
Equipment, tubulars and consumables	-	1.6
Sum		2.3

3.2.5.2. Above ground system

A two pipe concept (separate supply pipe and separate return pipe) has been selected. For the main part of the district heating network a DN50 pipe has been proposed. At the Earth buildings a split is made towards building A (DN 32) and building B (DN 40) Inside the building piping is needed from the building envelope to the technical room. The same diameter is selected for the inner piping circuit.

To deliver the heat to the building and to keep both circuits physically separated a heat exchanger is included both in building A (560 kW) as in building B (750 kW). Further, to circulate the water in the HOCLOOP concept and the district heating network piping a pump is integrated. To keep the pressure in the water circuit constant an expansion system is included (expansion of the water by increasing the temperature).

3.2.5.2.1. District heating network installed in the ground

Table 12 gives an overview of the costs for the district heating network installed in the ground. Besides the costs for piping also the costs for the dig works are included.

This project has received funding from the European Union's Horizon Europe research and innovation program under grant agreement No 101083558

Table 12. Overview of costs for district heating network at VITO if installed in ground.

District heating network in the ground	Length (meter)	Unit price (€/meter)	Total cost (k€)
DN50 insulated underground steel piping	834	223.65	186.5
DN50 dig works	834	55.00	45.9
DN32 insulated underground steel piping to building A	155	201.60	31.2
DN32 dig works	155	55.00	8.5
DN40 insulated underground steel piping to building B	48	207.90	10.0
DN40 dig works	48	55.00	2.6
DN32 insulated indoor steel piping in building A	26	186.30	4.8
DN40 insulated indoor steel piping in building B	26	186.30	4.8
Heat exchanger in building A			13.5
Heat exchanger in building B			18.0
Circulation pump			5.0
Expansion system			11.0
TOTAL			**342**

3.2.5.2.2. District heating network installed above ground

Table 13. Overview of the costs for the district heating network installed above ground. Besides the costs for piping also the costs for the electric tracing are included.

District heating network above ground	Length (meter)	Unit price (€/meter)	Total cost (k€)
DN50 insulated underground steel piping	834	265.50	221.4
DN50 dig works	834	80.00	66.7

This project has received funding from the European Union's Horizon Europe research and innovation program under grant agreement No 101083558

DN32 insulated underground steel piping to building A	155	207.00	32.1
DN32 dig works	155	80.00	12.4
DN40 insulated underground steel piping to building B	48	220.50	10.6
DN40 dig works	48	80.00	3.8
DN32 insulated indoor steel piping in building A	26	186.30	4.8
DN40 insulated indoor steel piping in building B	26	186.30	4.8
Heat exchanger in building A			13.5
Heat exchanger in building B			18.0
Circulation pump			5.0
Expansion system			11.0
TOTAL			**404**

3.2.5.3. Levelized costs of energy analysis

A financial analysis was conducted using the "CalDev" tool developed by IFPEN. This analysis enabled the determination of the cost of heat, based on the same assumptions as those applied to the Paris case. In particular, annual expenses related to operator salaries, maintenance, and insurance are estimated as a percentage of the CAPEX. For the reference scenario, considering a 20-year period, the Levelized Cost of Energy (LCOE) was estimated at 0.152 €/kWh. Importantly, this calculation includes the cost of transporting heat from the well, where the HOCLOOP system is installed, to the building. This component is case-specific and may not apply in situations where the well is drilled in the immediate vicinity of the building. In the present case, however, the well is an existing one, and neither its location nor that of the building was optimized. This constraint increases the transportation distance and therefore the calculated LCOE. In an optimized configuration, the LCOE would be expected to decrease.

3.2.6. Discussion

For the Belgian case, the HOCLOOP system is assumed to be installed in the existing well MOL-GT-03, with the objective of supplying the estimated heat demand of the new VITO buildings A and B. The demand is expected to fluctuate seasonally and daily between approximately 100 and 500 kW.

The cost of installing the system in the well is estimated at 2.3 M€, with an additional 300–400 k€ required to deliver the heat to the new buildings, located about 1 km from the well site. The configuration described in this section addresses heat demand only. The buildings also have a cooling demand, which would need to be met by a dedicated chiller system.

This project has received funding from the European Union's Horizon Europe research and innovation program under grant agreement No 101083558

As in the Paris case, a sensitivity analysis was performed to evaluate the impact of the system lifetime on the Levelized Cost of Energy (LCOE). The results, presented in Table 14, indicate that extending the project lifetime significantly reduces the cost of energy.

Table 14. Cost of energy for different project lifetime for the Belgium case

Project lifetime considered (yr)	10	20 (ref)	30	50
Cost of energy (€/kWh)	0.232	0.152	0.131	0.113

As in the French case, it should be noted that this temporal analysis is based on strong assumptions concerning the lifetime of technical components, as well as projections of energy prices, maintenance costs, and technological evolution.

The Belgian case is particularly constrained, since the locations of both the well and the buildings were predetermined and not optimal. Furthermore, the system is designed to deliver only heat, whereas the buildings also require cooling. Meeting this additional demand would require further investment in a chiller system. These factors make the business case for the HOCLOOP concept in this configuration less favorable. Currently an ATES system is installed near the buildings in order to deliver both heating (via a heat pump) and cooling.

3.3. German case study

3.3.1. Introduction

In Deliverable D4.2 [2], various simulations were conducted to assess the efficiency of the HOCLOOP solution for the Darmstadt case. The results indicate that a HOCLOOP system is not suitable for Darmstadt for two primary reasons. First, the local temperature gradient is relatively low. In 2023, three boreholes with SKEWs project (seasonal crystalline borehole thermal energy storage) were drilled to a depth of 750 m, with bottom-hole temperatures measured at 27 °C. This corresponds to a temperature gradient of 2.1 °C per 100 m—below the average value. Second, the rock type below surface is granite, which makes drilling cost high.

HOCLOOP's system targets locations with high temperature gradient, and the horizontal part should be located in a geological format that is easy to drilled. Both criteria cannot be met in Darmstadt. Therefore, after discussion with the project partner Reelwell and other project partners, it is not worth to investigate further, how to integrate HOCLOOP's solution in the district heating network and perform cost analysis.

However, an important feature of the HOCLOOP project is its dual pipe technology, developed by project partner Reelwell. Following consultation with the project consortium, priority should therefore be given to applying HOCLOOP's dual pipe technology to the medium-deep borehole thermal energy storage (MD-BTES) system in Darmstadt.

3.3.2. Current design of the borehole thermal energy storage system

At Campus Lichtwiese of TU Darmstadt, a first medium MD-BTES system was built within the framework of SKEWs project and being connected to the district heating network of TU Darmstadt within PUSH-IT project (https://www.push-it-thermalstorage.eu/). The system contains three 750 m depth borehole. It is planned that the borehole field should be extended to 19 or 37 boreholes in the future, depending on commitment from TU Darmstadt Figure 11.

This project has received funding from the European Union's Horizon Europe research and innovation program under grant agreement No 101083558

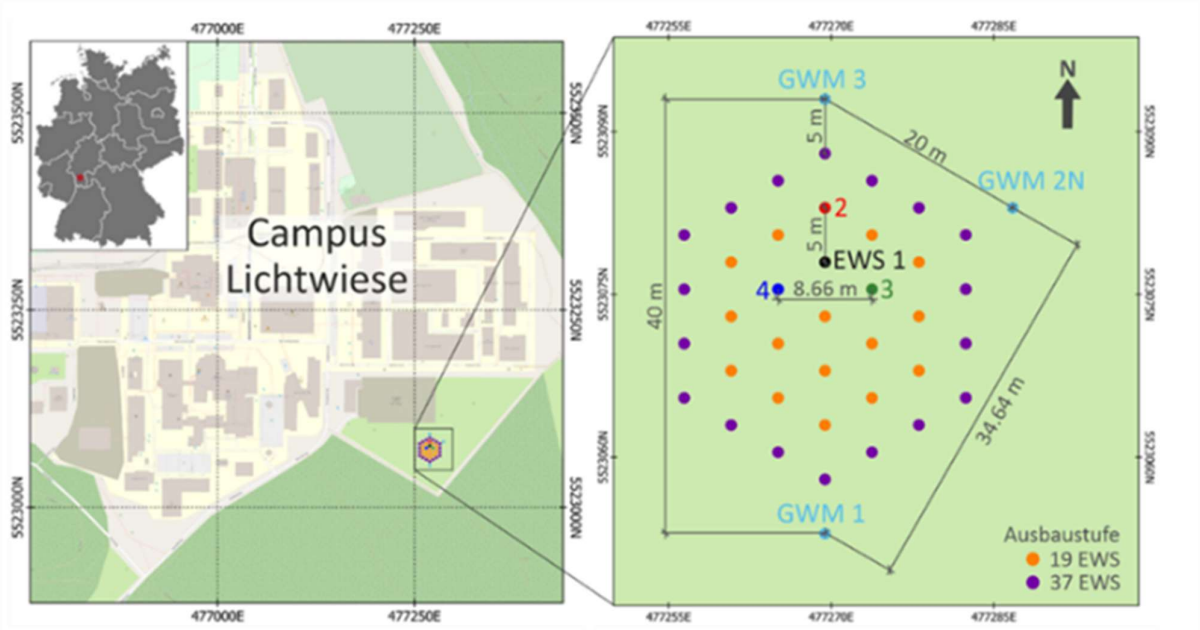

Figure 11. The MD-BTES system in Darmstadt with three boreholes (EWS2, EWS3, EWS4) and three groundwater monitoring wells (GWM1, GWM2, GWM3).

The boreholes have a diameter of 9 inches and are fitted with 7-inch steel casing. Inside this casing is 4.5-inch steel tubing lined with polypropylene (PPR) to provide thermal insulation (Figure 12). The working fluid is injected through the inner tubing, travels to the bottom of the borehole, and then returns upward through the annular space between the inner tubing and the outer casing.

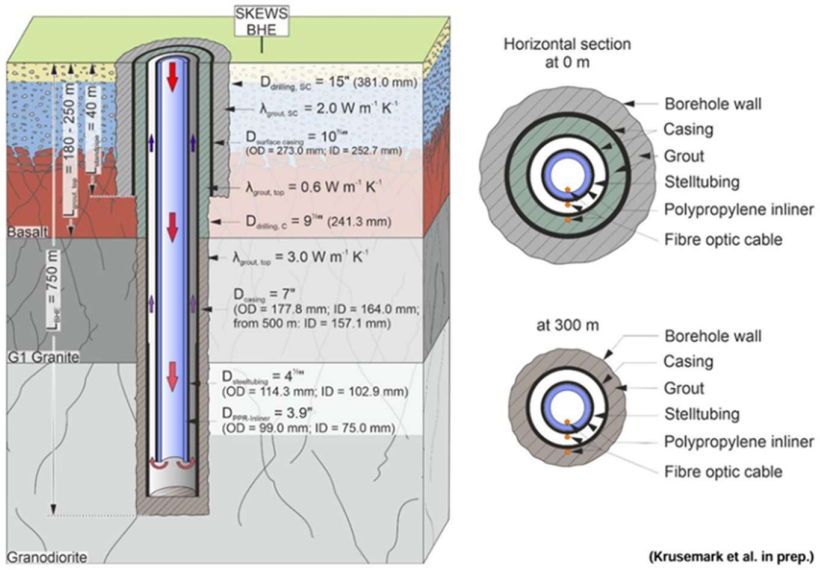

Figure 12. Cross-sections of a borehole.

In summer, hot water—sourced from waste heat generated by facilities such as CHP plants, solar collectors, or high-performance computing centres—is injected underground to store thermal energy. In

This project has received funding from the European Union's Horizon Europe research and innovation program under grant agreement No 101083558

winter, heat is recovered by circulating cold fluid through the system, supplying warmth to the campus.

3.3.3. HOCLOOP's casing for Darmstadt case

Within the HOCLOOP project, a key objective is to develop the Drill Heat String (DHS), in which the inner and outer casings are thermally insulated by a vacuum layer (Figure 13). This design significantly reduces heat loss caused by thermal exchange between the injected fluid and the returning fluid.

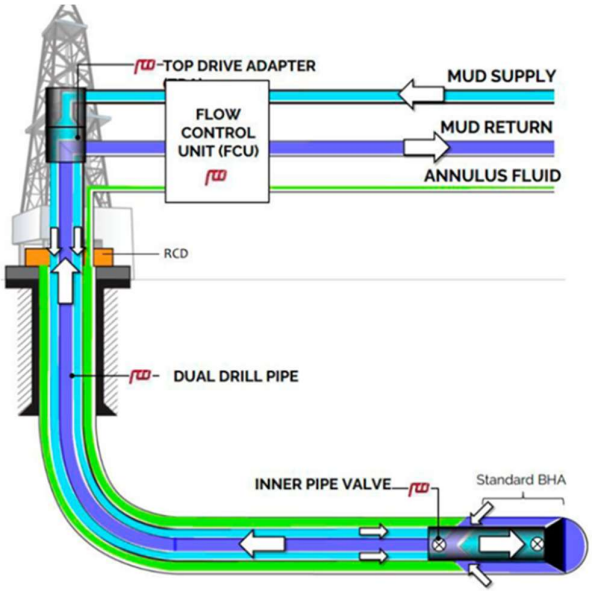

Figure 13. Drill Heat String of HOCLOOP system.

Compared with the PPR liner used in the MD-BTES system in Darmstadt, the vacuum-insulated inner casing offers several advantages. First, the thermal conductivity of a vacuum is much lower than that of PPR material, effectively minimizing heat exchange between the injected and outflow fluids. Second, PPR has a much higher thermal expansion coefficient, which requires installation gaps. In theory, these gaps should close at high temperatures; however, real-world tests have shown that they remain partially open, leading to heat loss (Seib et al., 2025). Finally, steel casings provide greater durability over time.

3.3.4. Compare current design and HOCLOOP's solution

3.3.4.1. Thermal efficiency

To assess the thermal efficiency of a PPR liner compared with a DHS system, two simulation models were developed. The first model contains 19 boreholes (Figure 14), and the second contains 37 boreholes (Figure 15), representing two possible future implementation scenarios. In both cases, the injection rate is set to 2 L/s per borehole. During the summer period (182.5 days), water is injected at 90 °C, followed by a winter extraction phase with an inlet temperature of 30 °C (also 182.5 days). Each model is simulated over a 30-year operational period.

For the PPR liner, the inlet pipe has a thermal conductivity of 0.4 W/m·K. For the DHS system with a vacuum layer, the combined equivalent thermal conductivity of the steel casing and vacuum layer is 0.0264 W/m·K.

Results (Figure 16 & Figure 17) indicate that, for the Darmstadt MD-BTES system, both the DHS and PPR liners yield nearly identical outlet temperatures in terms of thermal efficiency.

This project has received funding from the European Union's Horizon Europe research and innovation program under grant agreement No 101083558

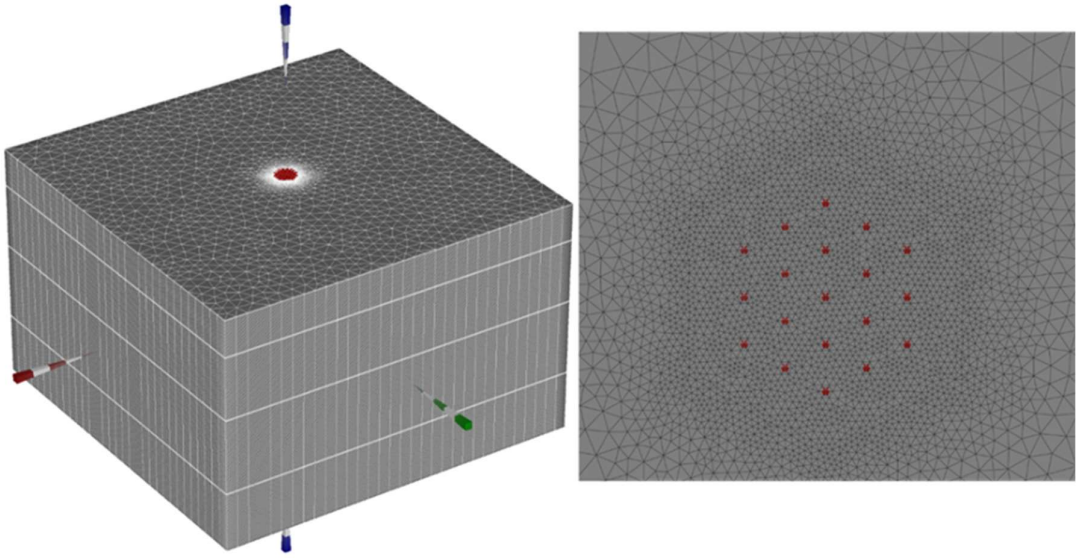

Figure 14. Model with 19 boreholes.

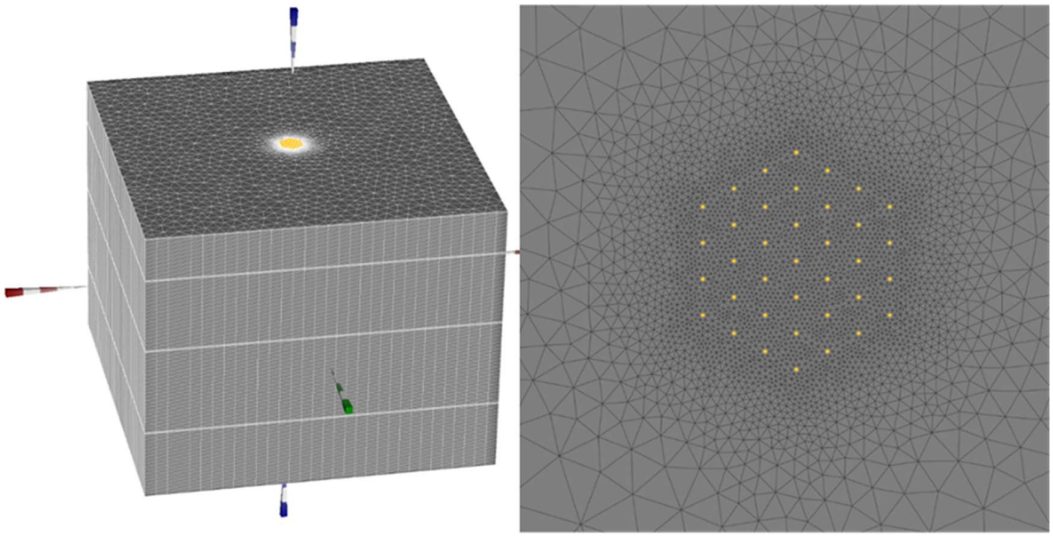

Figure 15. Model with 37 boreholes.

This project has received funding from the European Union's Horizon Europe research and innovation program under grant agreement No 101083558

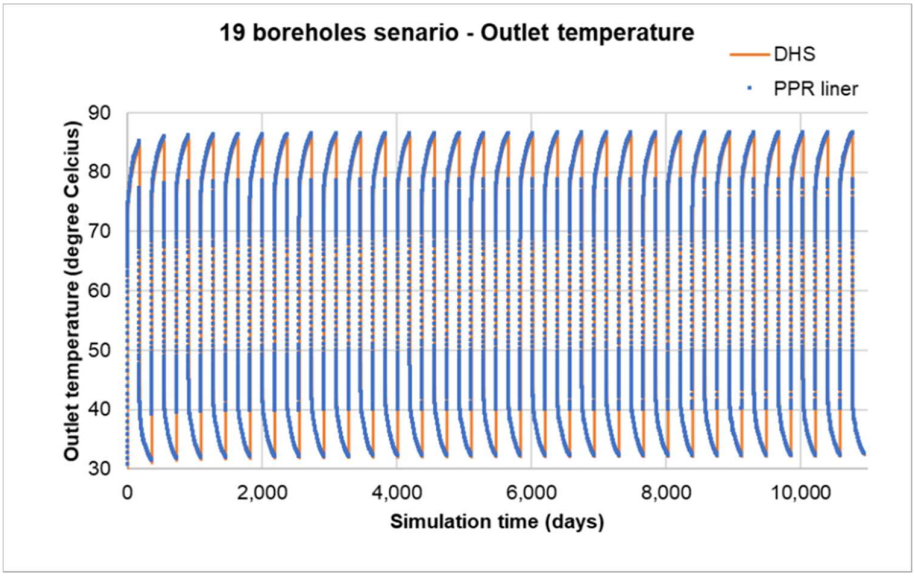

Figure 16. 19 boreholes scenario – Outlet temperature.

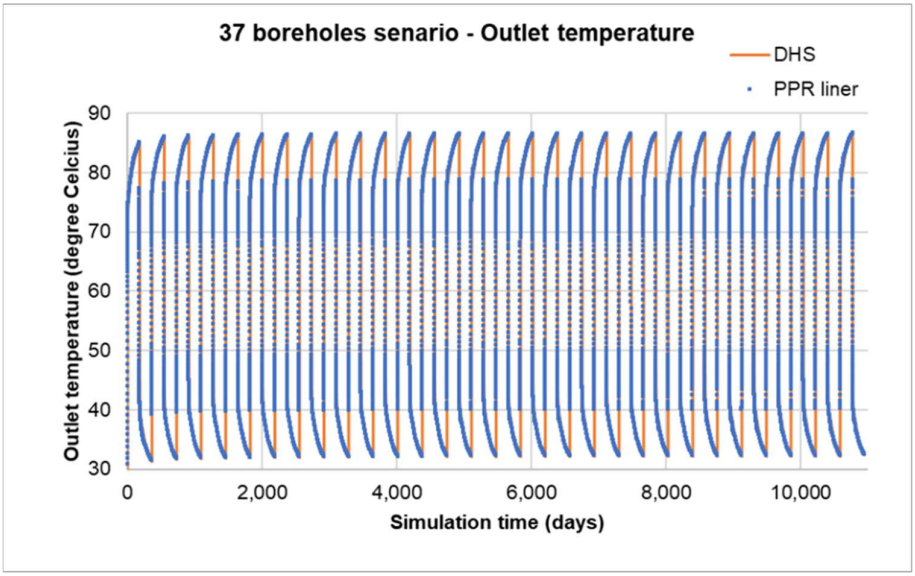

Figure 17. 37 boreholes scenario – Outlet temperature.

3.3.5. Cost comparison

Based on SKEW's project data, the material and installation of three PPR liners for three boreholes cost a total of 350 k€. This corresponds to approximately 116 k€ per borehole, excluding drilling and well completion costs.

For DHS, according to project partner Reelwell A.S., the total cost of installing a DHS in an existing 750 m-deep borehole is 400 k€—around 3.5 times the cost of a PPR liner.

3.3.6. Conclusion

For the Darmstadt case, the HOCLOOP system is not recommended due to unfavorable geological conditions and low temperature gradient. While the Dual pipe technology provides significant advantages in terms of durability and thermal insulation, the performance of DHS in the Darmstadt BTES system is

This project has received funding from the European Union's Horizon Europe research and innovation program under grant agreement No 101083558

comparable to that of the PPR liner, which is a much more cost-effective option.

3.4. Italian case study

3.4.1. Introduction

Previous deliverables [1] and [15] consist of all basic information about the Italian case study for the area of the Amiata and for the area of Gavorrano. For the sake of readability, the main information on the existing heating system in Gavorrano and Amiata is summarized below.

3.4.2. Integration of the HOCLOOP concept

The Gavorrano case is a district heating network (DHN) covering the town of Gavorrano and smaller town in the area powered by a set a of HOCLOOP wells while the Amiata case consists of a set of HOCLOOP wells that powers an Organic Rankine Cycle (ORC) and heats the greenhouses of an agricultural company. For further information on the details of the DHN and the ORC plant refer to (Fiaschi, et al., 2025) and previous deliverables (HOOCLOOP, 2023).

3.4.3. Coupled simulations

The results obtained have been showcased in previous deliverables, but for the sake of readability they are summarised. For the Gavorrano case, at least 10 wells are needed to obtain outlet temperatures over 85°C to supply the heat to the DHN operating between the temperatures 80-40°C as shown in Figure 18. The lower mass flow rate circulated in the case of higher number of wells allows to reach higher outlet temperatures and less depletion of the geothermal resource.

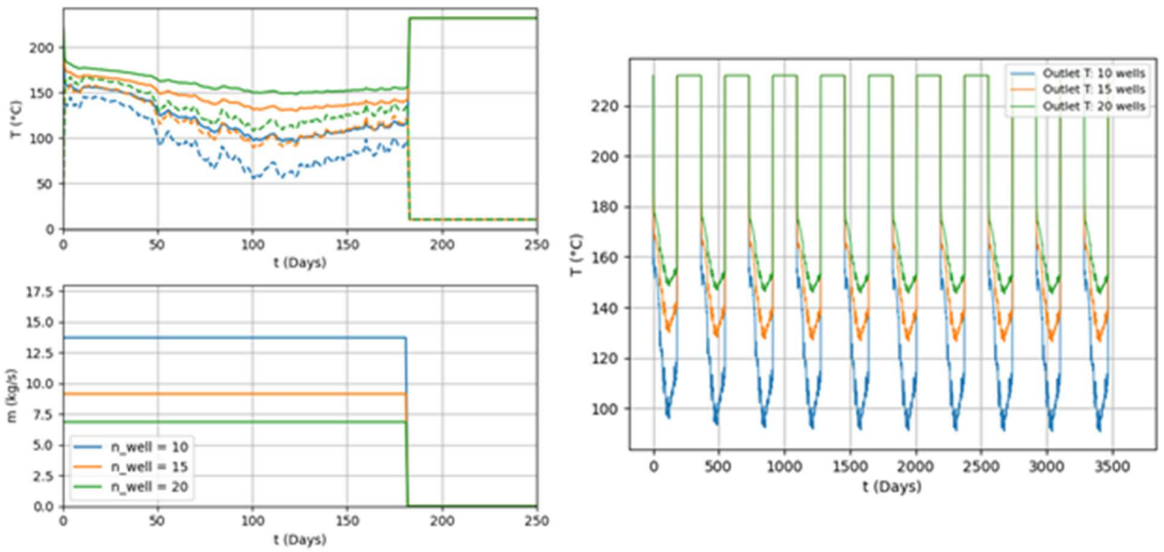

Figure 18. Outlet and inlet temperatures of the wells (top left)*; mass flow rate per well* (*bottom right*)*; outlet temperature over the years* (right).

For the Amiata case the obtained results are similar. The total mass flow rate needed is fixed monthly by the needs of the agricultural plants, for a certain number of well the total mass flow rate is divided equally between them. This means that for a lower number of wells the mass flow rate circulating is higher.

At least 15 wells are needed to provide the necessary heat to the agricultural plant throughout the years with an inlet temperature of at least 90°C. At the same time, in this configuration, the ORC does not

This project has received funding from the European Union's Horizon Europe research and innovation program under grant agreement No 101083558

operate often in fact it achieves a capacity factor (CF) of 0.18. If the number of wells is increased the CF of the ORC increases and for the case with 20 wells the CF improves to 0.6. This happens because the temperature at the outlet of the wells increases because the mass flow rate per well is less than for the case of 15 wells and consequently, the conditions at which the ORC plant operates are met more often. This also causes an increase in maximum power output of the well as show in Figure 19.

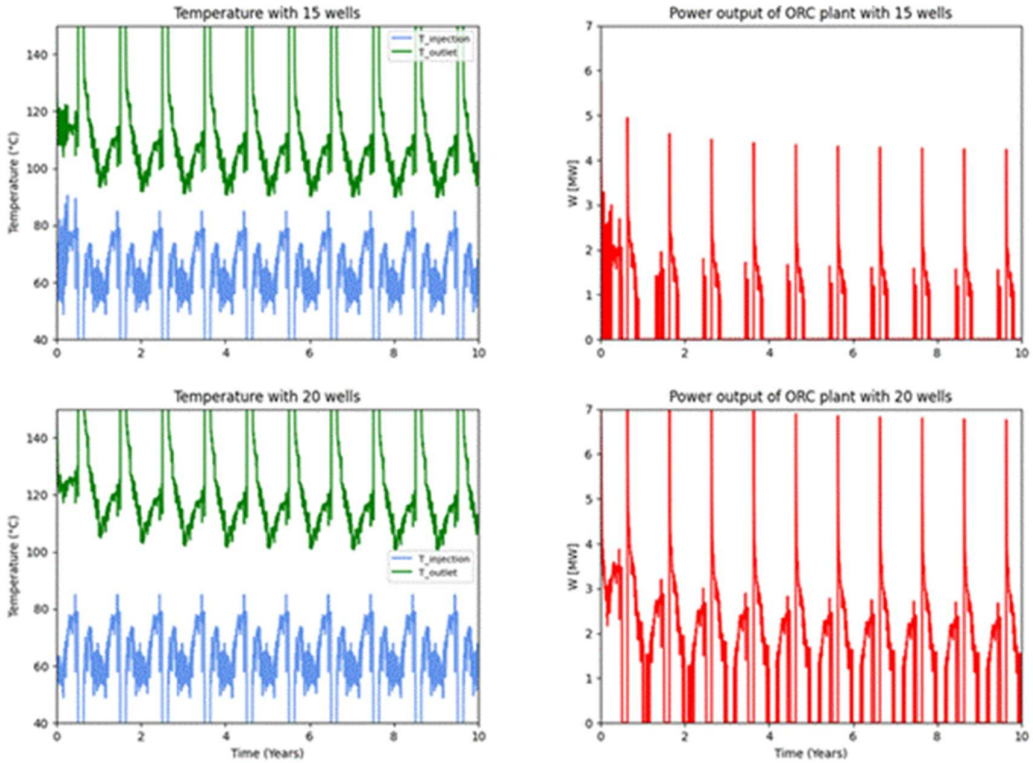

Figure 19. Outlet and inlet temperatures of the well for different number of wells (*left*) and *output power of the ORC plant* (*right*).

3.4.4. Cost analysis

The LCOE can be calculated using an approach like the one proposed by Ungar et al. [16]:

$$LCOE = \frac{C_{tot}\beta + \overline{\dot{W}_{tot}}}{\overline{\dot{Q}_{DH}}}, \beta = \frac{1 + \alpha OM_{ratio}}{\alpha h_y}, \alpha = \frac{1 + (1+i)^{-L_e}}{i} \quad (1)$$

where C_{tot} is the total investment cost predicted for the network, $\overline{\dot{Q}_{DH}}$ and $\overline{\dot{W}_{tot}}$ are the heating demand and the electrical power averaged over one year, OM_{ratio} is the annual rate of operation and maintenance cost taken as a percentage of the initial investment (assumed to be 5%), while L_e and i are respectively the life expectancy of the DHN (20 years) and the annual interest rate (4%). c_{el} = 11 c€/kWh was the average price of electricity in September 2025. Finally, h_y = 8760 h/year is the number of hours in a year. Notice that, for the Amiata case where a possible cogeneration is envisioned, the net power output can be in principle negative meaning that some electricity has been sold. This will reduce the overall *LCOE*, implicitly assuming that the focus of this plant is still the heat production with the additional selling of electricity considered mainly as an additional source of revenue. In the following the correlation employed for the evaluation of C_{tot} in both cases will be presented.

This project has received funding from the European Union's Horizon Europe research and innovation program under grant agreement No 101083558

3.4.5. Well cost estimation

For the calculation of well costs, two different approaches were adopted for the case studies. In the Gavorrano case, due to the relatively standard geological setting and the suitability of underground temperatures for traditional horizontal drilling steering bits, the drilling cost was directly estimated by Geotherma based on industry experience. Conversely, in the Amiata case, conventional horizontal drilling tools cannot be employed due to temperature limitations; therefore, Geotherma could not provide a reliable estimation. In this case, a standard correlation for drilling cost was applied to obtain a reasonable estimate of the overall system performance. For both sites, the cost of wells beyond the first was reduced by 30%, following Geotherma's recommendation, to reflect efficiency gains from increased expertise and geological knowledge. For the Gavorrano case, Geotherma cost estimation, divided in drilling, equipment and others, is shown in the table below. For a total of 10 wells needed in Gavorrano area to cover the need of the DHN the total cost for the installation of the HOCLOOP wells is 219 M€.

Table 15. Geotherma well drilling estimation for the Gavorrano case.

Cost item	Time	[M€]
Mob/Demob and site preparation	2 weeks +	2
Drilling and well operation (24/7)	6 months	16
Equipment, tubulars and consumables	-	12
Sum		30

For the Amiata case instead, the following cost correlation, developed for the genGEO tool by Adams et. Al. [16], has been used:

$$c_{well} = X_{IC-well} X_{PC-well} PPI_{O_G} \left(0.105 L_{well}^2 + 1776 L_{well} d_{well} + 2.753 * 10^5\right) \quad (2)$$

where L_{well} and d_{well} are respectively the overall length of the well and the outer diameter of the well in meter. The values of the other parameters are fixed and shown in the table below.

Table 16. Well drilling cost correlation parameters.

Parameter	Description	Value
$X_{IC-well}$	Contingency cost increase (assumed 15%)	1.15
$X_{PC-well}$	Indirect cost increase (assumed 5%)	1.05
PPI_{OG}	Inflation adjustment based on the oil and gas Producer Price Index [17] (reference is 2002 – the value shown is the correction factor for August 2025)	1.70

The overall cost of the well is then calculated as:

$$c_{welltot} = \frac{c_{well}}{s_{well}} \quad (3)$$

where s_{well} is the success rate of the well drilling. It allows to consider the possibility that the well drilled does not meet the expected performance or that something goes wrong in the drilling process and the well must be abandoned. For BHE and EGS this value can be considered of 0.90 [18] because the behaviour of

This project has received funding from the European Union's Horizon Europe research and innovation program under grant agreement No 101083558

the well is less dependent on the physical properties of the well, much higher than the 75% success rate for traditional geothermal systems.

In the Amiata area the wells drilled are assumed to be of length of 4700 m, divided in a vertical section of length 2200m and a horizontal section 2500 m long. The diameters for the vertical section and horizontal section are 24.4 and 21.7 cm respectively.

Applying the cost correlation a total cost per well of 17.3 M€ is obtained. Following the previous logic the cost of each well after the first one can be reduced by 30%, leading us to an estimate of 186.84 M€ for the configuration with 15 wells and an estimate of 247.39 M€ for the drilling of the configuration of 20 wells.

3.4.6. District heating network cost estimation

The plant installed in the area consists of a heat exchanger and pipelines to connect the wells to the towns. The correlations for the pipes and the heat exchanger are reported in the table below.

Table 17. Well drilling cost correlation parameters (all results are in $).

Component	Cost Correlation	Notes	Ref
Pipeline	$C_{pipe} = 0.6492\phi^{0.9779}L$	ϕ is pipe diameter [mm], L is pipe length [m]	[16]
Heat Exchanger	$\log_{10} C_{HE} = 4.6656 - 0.1557 \log_{10} A_{HE} + 0.1557[\log_{10} A_{HE}]^2$	A_{HE} is the heat exchanger area [m^2]	[20]
Pump	$\log_{10} C_p = 3.8696 + 0.3161 \log_{10} W_p + 0.1220[\log_{10} W_p]^2$	W_p is the power of the pump [kW]	[20]

The cost of the heat exchangers depends on its area, A_{HE}, which depends on the value of the overall heat transfer coefficient, U, and the mean logarithmic temperature difference, ΔT_{ml}. The heat transfer in the HE can be calculated from the following equation:

$$Q = UA_{HE}\Delta T_{ml} \quad (4)$$

To estimate the cost of the heat exchanger, the largest heat exchanger area has been taken as design conditions. The cost of each component is calculated with reference to the year 2002, to extrapolate the cost of the equipment today the value of Chemical Engineering Plant Cost Index (CEPCI) is considered. In particular, the CEPCI value of January 2024 is considered, and it is scaled by the reference value of the year 2002.

$$C_{year} = C_{ref_{year}} \frac{CEPCI_{year}}{CEPCI_{ref_{year}}} \quad (5)$$

3.4.7. ORC plant cost estimation

Following the approach employed for the previous Deliverable (D4.2) [2], instead of directly solving the ORC together with the well, a correlation has been developed to relate the cost of the ORC to the result of the well calculation.

Starting from the optimal design point identified in the previous deliverable, the correlation of the cost has been derived to account for possible changes in well flow rate and inlet temperatures which will have an

This project has received funding from the European Union's Horizon Europe research and innovation program under grant agreement No 101083558

impact on the heat exchanger and turbine sizing. The cost of the component, have been evaluated following the correlations developed by Turton et al. [20], which usually has the following form:

$$C_x = Cepci 10^{K_1 + K_2 \log_{10} x + K_3 [\log_{10} x]^2} \quad (6)$$

where C_x is the cost of the component, x is the scaling factor for the specific component (area of the heat exchangers, turbine power etc.), *Cepci* is a corrector to consider the inflation effect based on the *Chemical Engineering Plant Cost Index* (the reference is Jan. 2002).

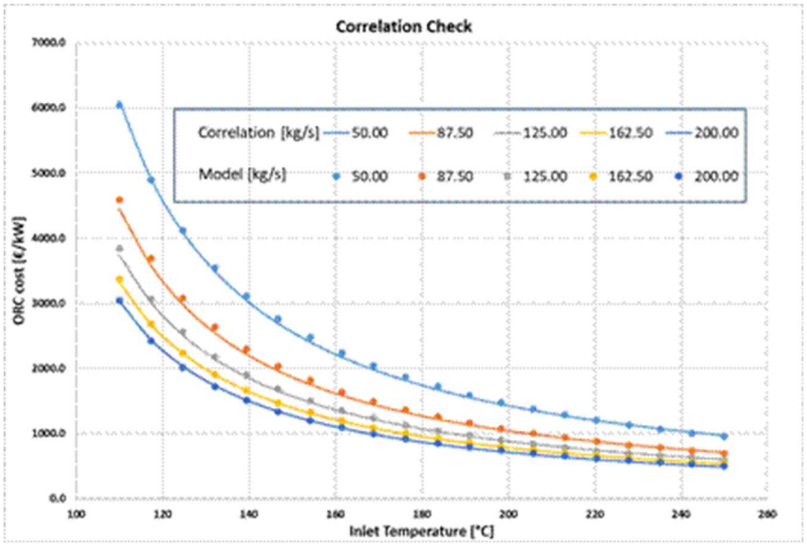

Figure 20. Relative cost correlation for ORC plant.

The cost of the power plant has been evaluated for different well flow rates (*range*: 50-200kg/s) and well output temperature (*range*: 110-250°C). The results, shown in Figure 18, have been used to develop a correlation for the relative price of the ORC (in €/kW). The developed correlation has the following form:

$$c_{rel} = A \left(\frac{t_{in}}{t_{ref}} - 1 \right)^{a_1} \left(\frac{m_{well}}{m_{ref}} - 1 \right)^{a_2} \quad (7)$$

The resulting correlation parameters are shown in the table below. Following the same approach used for the Gavorrano case's heat exchangers, the correlation has been evaluated over all the off-design condition and the worst condition (namely the highest cost) has been considered as the design one assuming that, in this way all the other conditions can be met.

Table 18. ORC plant cost correlation parameters.

Parameter	Value
A	3000 €/kW
a_1	-1.14
a_2	-0.39
t_{ref}	75 °C
m_{ref}	20 kg/s

This project has received funding from the European Union's Horizon Europe research and innovation program under grant agreement No 101083558

3.4.8. Discussion

In this section are analysed the results of economic analysis of the Gavorrano District Heating Network and of the Amiata Plant.

3.4.8.1. Gavorrano case

The ΔT_{ml} decreases over time because the outlet temperature decreases with time because of the depletion of the geothermal resource. This results in an increase in area of the heat exchanger to achieve the same result which consequently consists in an increase in costs.

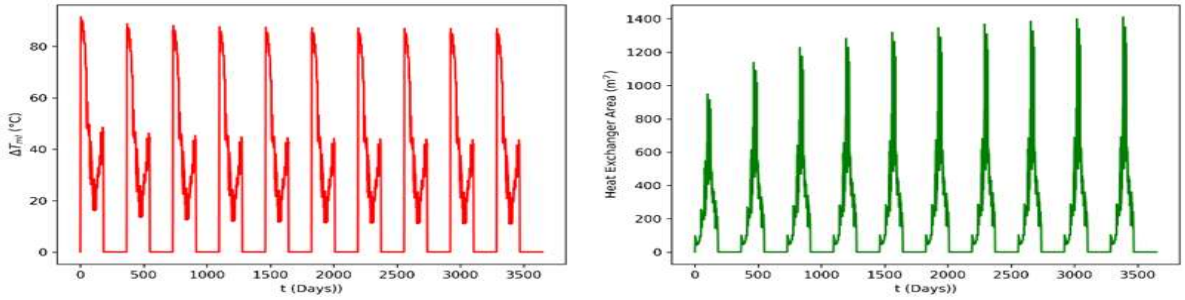

Figure 21. Variations of ΔT_{ml} over time and relative variation of heat exchanger area.

The overall initial capital cost consists mainly in the cost of the drilling and installation of the wells, covering up to 96.1% of the total cost while the installation of the DHN covers the remaining 3.9%. Applying the formula in equation (1) the *LCOE* obtained is 0.2688 €/kWh.

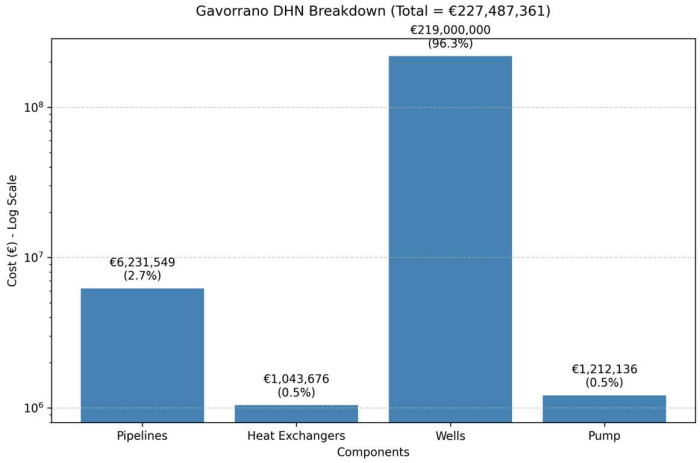

Figure 22. Breakdown of component costs of the Gavorrano DHN

3.4.8.2. Amiata case

The capital investment cost for the area of Mount Amiata consists in the costs of the well, the ORC plant and pipelines to connect the wells to the power plant and the agricultural industry. No additional costs are assumed for the use of the heat as the plant already exists.

In the economic evaluation of this area both the case with 15 and 20 wells are analysed. While the price of the wells, pipelines and heat exchangers are fixed, the power of the ORC and the inlet conditions vary

This project has received funding from the European Union's Horizon Europe research and innovation program under grant agreement No 101083558

making the price fluctuate while matching the conditions of the wells and overall, it decreases with time.

For both cases the maximum cost is achieved at the beginning of use of the plant.

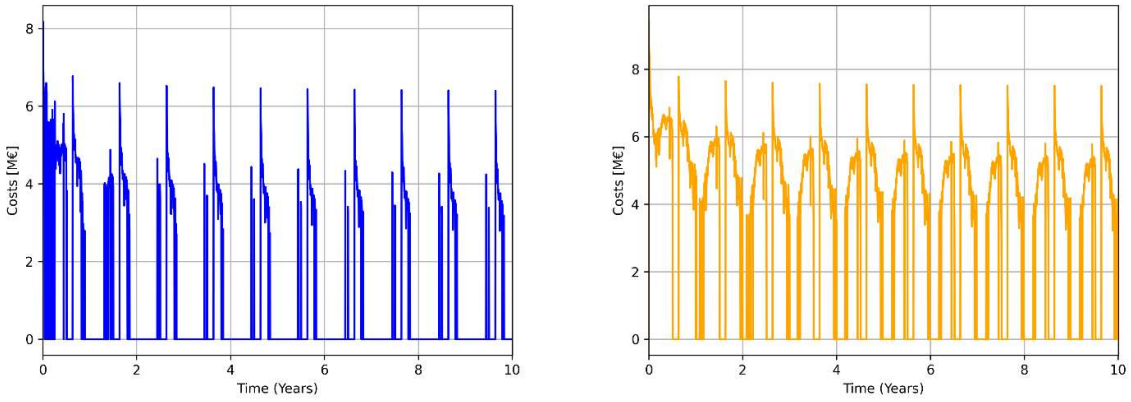

Figure 23. Cost of the ORC power plant over time for the configuration with 15 wells (left) and 20 wells (right).

The bigger number of wells increases the maximum size and cost of the ORC plant as the output power of the well increases. In both cases the biggest percentage of the investment resides in the cost of drilling and installation of the wells, which is around 95% in both cases.

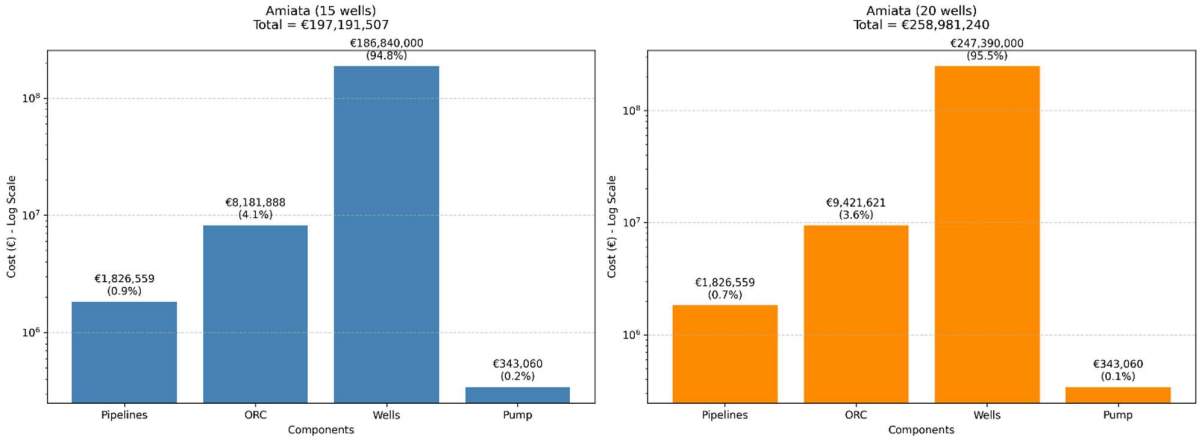

Figure 24.Breakdown of component costs of the Amiata Plant

Similarly, as the previous case the same equation is used to evaluate the *LCOE*. Here the heating demand is the demand of the agricultural plant while the electrical power $\overline{\dot{W}_{tot}}$ is the net difference between the circulation pump and the ORC average power outlet. Due to the reduced cost of installations of the wells in this site the *LCOE* is much lower that for the DHN in Gavorrano. In fact, for the case of 15 wells the *LCOE* achieved is $LCOE_{15}$ = 0.07763 €/kWh while for the case of 20 wells it is $LCOE_{20}$ = 0.09622 €/kWh.

The increase in ORC power output, due to the increased number of wells, does not provide enough energy to lower the *LCOE* of the plant as it brings along a substantial increase in capital costs. For the case with 20 wells, the electrical energy produced would need to be sold at an incentivized price (c_{el} = 0.524€/kWh), higher than the market price, to achieve the same *LCOE* as in the case with 15 wells.

Overall, the economic feasibility of this kind of systems heavily depends on the cost of drilling and installation of the wells since it is the most relevant cost and on the quality of the geothermal resource. In

This project has received funding from the European Union's Horizon Europe research and innovation program under grant agreement No 101083558

the Amiata case, the favorable geothermal gradient allows for the deployment of shorter wells, which reduces drilling and installation costs. As a result, the LCOE for the Amiata Plant is lower than that of the Gavorrano DHN.

3.5. Polish case study

3.5.1. Introduction

Previous deliverables include all basic information about the Polish case study, the area of Goleniów city [1, 2]. For the sake of readability, the main information on the existing heating system in Goleniów is summarized below.

3.5.2. District heating network

The information about the district heating in Goleniów are based on D4.2 [2], but it was updated in July 2025. The following information updates the data on the heating system in Goleniów with new information obtained directly from the operator in September 2024. Goleniów is a city with a population of 19550 citizens based on the official information published on the Facebook page of Goleniów Municipality (Goleniów Municipality, 2025). In the case of Goleniów, the district heating and the largest energy source operator is Goleniowskie Przedsiębiorstwo Energetyki Cieplnej (PEC Goleniów, 2025). The heating station is located in Goleniów at Maszewska 18 street (Figure 25, Figure 26 and Figure 27).

Figure 25. The area of the heat source PEC Goleniów, marked yellow dashed line [19].

The heat carrier for the mentioned energy source is hard-fine coal, and one boiler is adapted to burn biomass in the form of wood chips with a power 6 MW. Biomass can also be co-fired with coal. The installed capacity at the source is 29.26 MW, comprising 2 x 11.63 MW of coal-fired boilers (type WR-10, manufactured in 1981, with a thermal efficiency of 78%) and 6 MW of biomass and coal boiler (type WR-6, with an efficiency of 85%) (Atmoterm S.A., 2022). The efficiency of exhaust gas dust removal is 93%. The

This project has received funding from the European Union's Horizon Europe research and innovation program under grant agreement No 101083558

heat carrier in the heating network is circulating water with a pressure of 1.6 MPa. The network is designed for 135/70°C (based on the power control table in the heating season 2023/2024, shared by PEC Goleniów). The nominal flow of water is 263 Mg/hr (~263 m³/hr). The amount of heat distributed (sold) by the district heating in Goleniów commune is estimated at 165 468 GJ/yr in 2023 (based on a request sent to PEC Goleniów in September 2024). Energy production by the energy source at that time was 201618 GJ/yr. The efficiency of energy delivery can be estimated at 82%. In 2023, the ordered power for heating was 18.7 MW, and for hot tap water, it was 4.1 MW. The non-renewable primary energy input factor for the PEC Goleniów installation is Wpc = 1.6056 (direct information delivered by PEC Goleniów, September 2024 by email).

Figure 26. The area of the heat source PEC Goleniów, marked yellow dashed line [19].

Figure 27. Orthophoto map of the area, taking into account the course of the heating system and the location of buildings. The area of the PEC Goleniów marked by yellow dashed line [19].

3.5.2.1. The current price of energy

Heat from the PEC Goleniów

The settlement tariff regulates financial settlements for generating and supplying heat energy (PEC Goleniów heat tariff, 2024). The sale of heat is based on four tariff groups: A1, A2, A3, A4. In all cases, the heat is delivered by a heating station at 18 Maszewska Street in Goleniów. The significant difference between the groups is: the users' location, the property of the connection node elements and their type.

This project has received funding from the European Union's Horizon Europe research and innovation program under grant agreement No 101083558

The original currency in Table 19 is PLN (Polish Zloty), and it is recalculated to €. Based on the Polish National Bank, the exchange ratio PLN to € in the recent year can be estimated as 1 € = 4.25 PLN Figure 28.

Figure 28. Exchange ratio € - PLN in one year, in the time period May 2024 – May 2025 [20].

The installed thermal capacity of the energy installation in the case of PEC Goleniów exceeds 20 MW, so it is obligated to participate in the EU Emissions Trading System (EU ETS). The average yearly price of CO2 emissions in the last year can be estimated as 69.92 €/Mg_{CO2} (Figure 29).

Figure 29. Yearly variation of CO2 emission price in [€/MgCO2] [21].

This project has received funding from the European Union's Horizon Europe research and innovation program under grant agreement No 101083558

Table 19. Heat tariffs in the case of PEC Goleniów (PEC Goleniów, 2025) net values (VAT excluded).

Type of payment	Unit	Group A1	Group A2	Group A3	Group A4
Ordered power	PLN/(MW yr) €/(MW yr)	247721.92 58287.51	247721.92 58287.51	247721.92 58287.51	247721.92 58287.51
Price of heat production	PLN/GJ €/GJ	53.91 12.69	53.91 12.69	53.91 12.69	53.91 12.69
Price of heat carrier *	PLN/m^3 €/m^3	63.61 14.97	63.61 14.97	63.61 14.97	63.61 14.97
Constant part of heat power delivery	PLN/(MW yr) €/(MW yr)	49436.93 11632.21	83008.02 19531.30	59169.54 13922.25	92867.42 21851.16
Variable part of heat delivered	PLN/GJ €/GJ	23.02 5.42	29.86 7.03	20.64 4.86	30.42 7.16

* Important only if anyone can buy treated (district heating quality) water, e.g., filling an installation with water.

Assuming the emission of CO_2 factor 94.83 kg/GJ (KOBiZE, 2023), the cost of energy, which includes only the CO2 emission price, can be estimated as:

$$eCO2 := 69,92\ \frac{€}{Mg}\ 94,83\ \frac{kg}{GJ} = 6,63\ \frac{€}{GJ}$$

$$eCO2 = 28,18\ \frac{PLN}{GJ}$$

It is more than half the energy production price (Table 19). The cost of hard coal (culm) in the area of Goleniów can be estimated as 960-1280 PLN/Mg (lower caloric value ~21 MJ/kg) [22], assuming burning efficiency 0.82 (typical for the type of units used in the heating station) the variable cost of energy obtained, including only price of energy carrier can be estimated as follows:

$$e_{coal} := \frac{960\ \frac{PLN}{Mg}}{0,82 \cdot 21\ \frac{MJ}{kg}} = 13,12\ \frac{€}{GJ}$$

$$e_{coal} = 55,75\ \frac{PLN}{GJ}$$

It slightly exceeds the energy production price in PEC Goleniów. The variable energy production cost, including fuel and CO_2 emission, should exceed 60 - 70 PLN/GJ (14.11 - 16.47 €/GJ), depending on the share of the free of charge CO_2 emission. To confirm this thesis, we can cite the current prices of energy production in other installations using the same energy carrier, e.g.:

- MPEC Kraków [23] 73.69 PLN/GJ (net),
- Veolia Energia Łódź [24] 60.58 PLN/GJ (net),
- Geotermia Koło (energy produced based on coal plus biomass so far) [25] 63.90 PLN/GJ.

If the full constant price of energy includes the constant and variable cost of energy production, it can be

This project has received funding from the European Union's Horizon Europe research and innovation program under grant agreement No 101083558

estimated as follows:

$$c_{constant\_PEC\_Goleniow} := 53,91\ \frac{PLN}{GJ} + 247721,91\ \frac{PLN}{MW\ yr} = 61,76\ \frac{PLN}{GJ}$$

$$c_{constant\_PEC\_Goleniow} = 14,53\ \frac{€}{GJ}$$

Users are not able to utilise the full ordered power for a whole year (standard value of yearly load factor LF under Polish climatic conditions is 0.25), because the real energy price of energy for them can be estimated as follows:

$$c_{constant\_PEC\_Goleniow} := 53,91\ \frac{PLN}{GJ} + \frac{247721,91\ \frac{PLN}{MW\ yr}}{0,25} = 85,31\ \frac{PLN}{GJ}$$

$$c_{constant\_PEC\_Goleniow} = 20,07\ \frac{€}{GJ}$$

Finally, the energy price originating from PEC Goleniów is assumed to be 61.76 PLN/GJ (14.53 €/GJ). We exclude the transmission costs because in the case of geothermal energy, we are going to utilise the same infrastructure.

3.5.2.2. Electricity from the national electricity grid

The price of electricity is strongly dependent on the supplier and negotiated terms. The main electricity suppliers in the area covered by the analyses are PGE (Polish Energy Group) and E.ON. The price of electricity applicable to the final customer, including all fee components, excluding VAT, can be assumed at PLN 1.2/kWh (i.e. PLN 333.33/GJ) [26]. The source states PLN 1.17/kWh for E.ON and PLN 1.19/kWh for PGE, prices from 2025 [27]. Higher net value, 1.19 PLN/kWh=0.28 €/kWh (77.78 €/GJ), will be adopted in further calculations.

3.5.2.3. Heat obtained from natural gas

Natural gas prices depend on several factors, including consumption and contracted capacity. However, generalising somewhat, it can be estimated at approximately. PLN 3.4/m^3 net, taking into account all tariff components (calculations were made based on the calculator provided by PGNiG (PGNiG, 2025), assuming consumption of 103, 104, 105, 106, 107 m^3/month, the gas had a upper calorific value of 39.65 MJ/m^3, for the given consumption the following unit gas prices were obtained in [PLN/m^3] net: 3.77; 3.43; 3.40; 3.39; 3.39). In further calculations, a unit price of gas of PLN 3.4/m^3 net will be assumed for gas with an upper calorific value of 39.65 MJ/m^3 and a lower calorific value (determined by calculation) of 35.64 MJ/m^3. The price of energy from gas calculated with this assumption would be approximately.:

$$c_{gz} := \frac{3,4\ \frac{zł}{m^3}}{0,9 \cdot 35,64\ \frac{MJ}{m^3}} = 106\ \frac{zł}{GJ}$$

That is net about 24.94 €/GJ, OPEX only included. In the case of natural gas, CAPEX includes maintenance and depreciation of fixed assets (a boiler, chimney), giving additionally ~4.5 €/GJ net. The total net price of heat from natural gas can be estimated as 29.44 €/GJ.

3.5.2.4. The price of connection pipelines

This project has received funding from the European Union's Horizon Europe research and innovation program under grant agreement No 101083558

The heat tariff also includes the price of a double pipe connection between a user and the district heating. The value can be helpful in the estimation of a connection price – Table 20. Surprisingly, the connection cost is much lower than the price of pre-insulated pipes (just pipes, excluding assembling, and other fees). The price of pre-insulated pipes, based on [28], is listed below Table 20, net price for 6 m long sections, single pipe.

Table 20. Price of pre-insulated pipes [29].

DN [mm]	Net price, single pipe 6 m length section [PLN]
32	689
40	759
50	932
65	1200
80	1362
100	1774
139	1865
168.3	2240

The price of connection pipelines was estimated based on the double pipe price times 1.3. The factor 1.3 includes the installation costs.

Table 21. Financial expenditures in a case of double pipe connection between a user and district heating (net values).

no	Diameter nominal [mm]	Length up to 10 m in the open space [PLN/m / €/m]	Length up to 10 m in the in partially paved terrain [PLN/m / €/m]	Length higher than 10 m in the open space [PLN/m / €/m]	Length higher than 10 m in the in partially paved terrain [PLN/m / €/m]
1	DN100	730 / 171.77	750 / 176.47	109 / 25.65	143 / 33.65
2	DN80	570 / 134.12	600 / 141.18	86 / 20.24	115 / 27.06
3	DN65	480 / 112.94	490 / 115.29	66 / 15.53	93 / 21.88
4	DN50	410 / 96.47	440 / 103.53	61 / 14.35	85 / 20.00
5	DN40	350 / 82.35	370 / 87.06	54 / 12.71	76 / 17.88
6	DN32	300 / 70.59	320 / 75.29	51 / 12.00	73 / 17.18
7	DN25	280 / 65.88	300 / 70.59	44 / 10.35	65 / 15.29

The price list of pipeline connections refers to small diameter, based on the price list of pipes [30] , it can be estimated that the price of the connection.

This project has received funding from the European Union's Horizon Europe research and innovation program under grant agreement No 101083558

The distance from the main heating plant of PEC Goleniów to the zone of the salt dome can be estimated to be approximately 12.1 km straight (Figure 30). Considering a more realistic route along traffic routes (roads), it can be approximately 18 km. The pipe's diameter depends on the energy carrier's flow rate, which in turn depends on the number of HOCLOOP units assumed to be optimal – a task for further work in the report. In the case of the salt pillow, the distance between the central heating station and the structure in a straight line is about 4.8 km (Figure 33), following a similar assumption that we will go closer to the salt pillow by subsurface district heating pipes, going along roads, the length of the connection will be identical. The Goleniów Airport is situated above the salt pillow; photos of the object are in Figure 31 and Figure 32.

3.5.2.5. Estimated power and heat demand in the case of Goleniów Airport

The total area covered by the airport buildings can be estimated as 5,700 m² (based on planimetric measurements of the orthophoto map of the object performed in the geoportal2.pl), and the height of the buildings is approximately 7 m (mean), which yields a cubature of 39,900 m³. Typical power demand for a multi-family new building (built after 1997) can be estimated as 11.5 W/m^3 - based on (Szkarowski, 2012). Based on the Airport's fitting of that rule, the power demand can be calculated as 460 kW, corresponding to an energy consumption of approximately 3 620 GJ/yr. A small local heating network is available in the airport area. The facility is heated by natural gas from a local energy source.

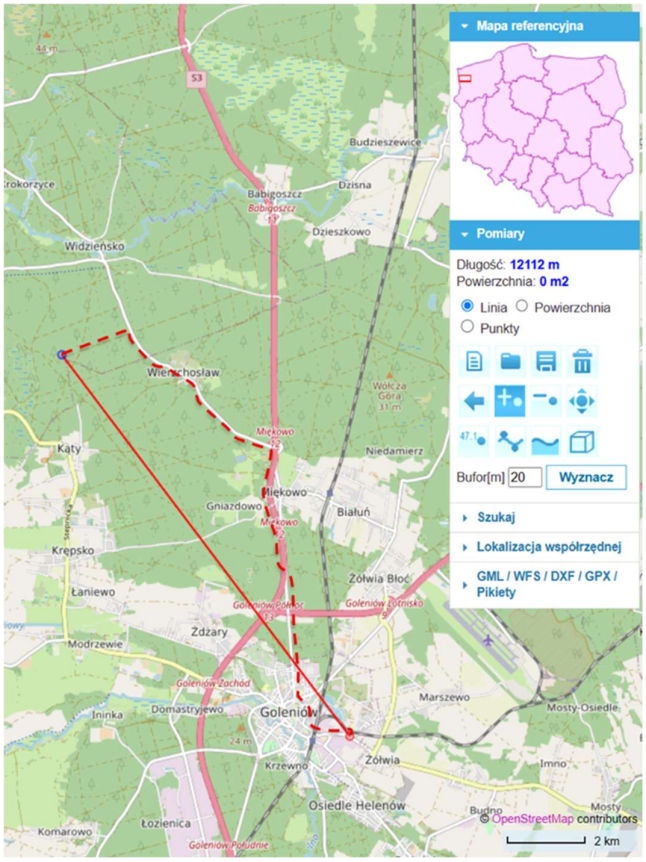

Figure 30. The straight-line distance from the PEC Goleniów heating plant, at ul. Marszewska 18 to the center of the salt dome based on www.geopoertal2.pl is estimated at 12.1 km. A more probable route of the pipeline, assuming its laying along the traffic routes, marked with a red dashed line, has a length of approx. 18 km.

This project has received funding from the European Union's Horizon Europe research and innovation program under grant agreement No 101083558

Figure 31. General view of the Goleniów Airport [31].

Figure 32. Goleniów Airport, departure zone 3500 m^2, arrival zone 800 m^2, the main hall 1000 m^2 [32].

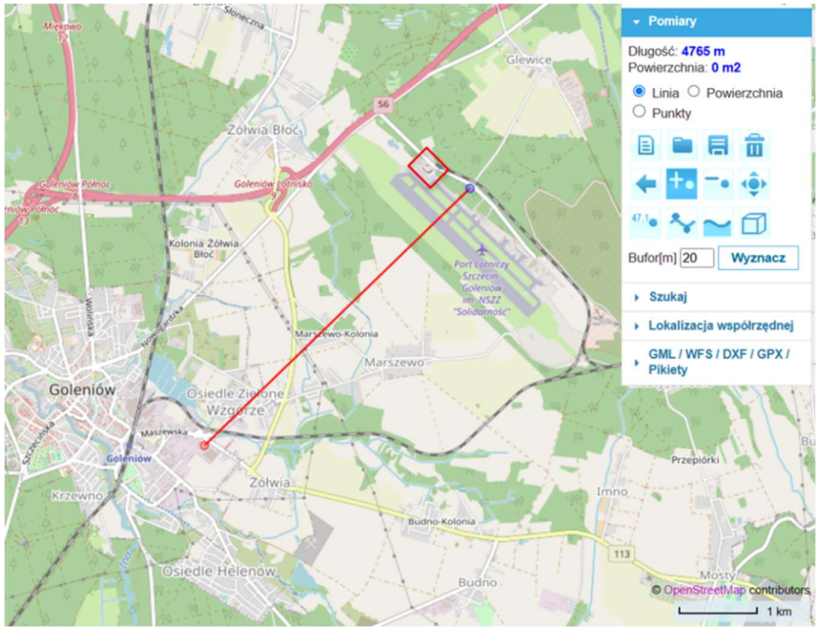

Figure 33. The straight-line distance from the PEC Goleniów heating plant is marked red solid line, at ul. Marszewska 18 to the center of the salt pillow, based on www.geopoertal2.pl estimated at 4.8 km. The location of alternative path for connection pipe is marked red dashed line, the length is similar ~4.8 km.

This project has received funding from the European Union's Horizon Europe research and innovation program under grant agreement No 101083558

3.5.2.6. Meteorological data (TMY)

Calculations based on meteorological data represented by the Typical Meteorological Year were generated using data from the period 2005-2020, employing the SARAH3 algorithm, supported by the Photovoltaic Geographical Information System (EU Science Hub, 2024). However, in July 2025, an updated version of meteorological data was published (covering the time period 2005-2023). The authors decided to use those available when the previous deliverable was elaborated, 2005-2020. It allows us to use all the technical calculations that were done previously. The minimal outlet temperature recorded in Goleniów, following the TMY, was higher than suggested by the design standard (PN-EN-12831, 2006), that is -16°C in the case of Goleniów. Since the original TMY, the lowest noticed temperature was corrected to reflect the lowest noticed value of ambient air, which was changed to -16 °C. Temperature and relative humidity versus time during the heating season are presented in Figure 34. Assuming a thermal definition of the beginning and end of the heating season as the period that begins when the average daily air temperature is lower than 10°C (beginning) or higher than 10°C for three days in a row, assuming that internal gains allow heating of buildings from an outside temperature of 12°C. The average air temperature in the heating season is 2.6°C, and its length is 187 days.

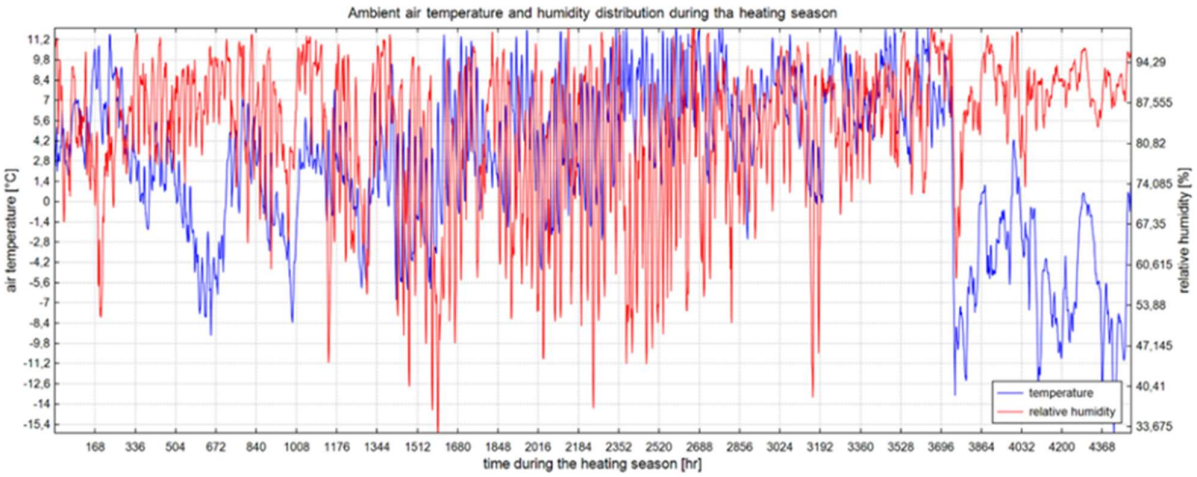

Figure 34. Ambient air and relative humidity during a heating season in the case of Goleniów, based on TMY PVGIS-SARAH3(2005-2020).

3.5.2.7. Estimation of financial expenditures for the HOCLOOP unit

Financial spending in the case of a single unit of HOCLOOP has been estimated by the project consortium member (REELWELL), based on certain assumptions, at 21 M€. That includes 2 M€ for mobilisation and demobilisation of a drilling site, 8 M€ for drilling and well operation and 11 M€ for equipment, tubulars and consumables. That gives a constant part of the drilling 2 M€ plus 19 M€, depending on the borehole heat exchanger length (6800 m). It can be assumed that the HOCLOOP unit cost $k_{HOCLOOP}$ [€] with a specific length $h_{HOCLOOP}$ [km] can be estimated as:

$$k_{HOCLOOP}\ [M€] = 2\ M€ + h_{HOCLOOP}\ [km] * 2.794\ M€/m$$

Unitary ordered power price in the case of HOCLOOP based only on financial expenditures and lifetime of the borehole heat exchanger utilisation can be estimated based on the cost of the HOCLOOP unit and obtained power ~1.6-1.8 MW (average 1.7 MW) – estimated in technical calculations done in the deliverable D4.2 (Hernandez, et al., 2025) in the case without heat pump, assuming flow of energy carrier

This project has received funding from the European Union's Horizon Europe research and innovation program under grant agreement No 101083558

20 m³/h:

$$C_{constant\_HOCLOOP} := \frac{\frac{21 \cdot 10^{6}\ €}{30\ yr}}{1,7\ MW} = 1,75 \cdot 10^{6}\ \frac{PLN}{MW\ yr}$$

That is seven times higher than currently, but the variable energy price will be negligible without using heat pumps.

3.5.3. Coupled simulations

Cases related to the salt dome are marked as SD, while cases related to the salt pillow are marked as SP. In the case of the salt dome, the heating plant manages the energy obtained by HOCLOOPS' units. In the case of the salt pillow obtained by HOCLOOPS' units, energy can be utilised directly by both the heating plant and the Airport. Variants linked with the heating plant are marked by "hp", and those connected with the Airport are marked by "ap". In the previous deliverable D4.2 done in the scope of the HOCLOOP project (Hernandez, et al., 2025), two variants of coupling HOCLOOP units were examined, with and without heat pumps: Figure 35 and Figure 36. It was concluded that in the Polish case, utilisation of heat pumps allows a significant reduction in the share of energy originating from coal, from about 115 TJ/year (Figure 106 in the cited report) to about 90 TJ/year (Figure 108 in the cited report). Bearing in mind the target of decarbonisation of the Polish energy sector, the variant that allows for a reduction in energy originating from coal seems to be more promising. Because the subject of this report is the financial optimisation of the energy source, both possibilities were considered. The preference decision depends on the amount of energy heat pumps produce in a specific case. However, the rough financial profitability of heat pump utilisation can be calculated for both heat sources based on the minimum COP value required to reach heat pump profitability, which is:

- in the case of the heating plant operated by PEC Goleniów

$$COP_{min\_Airport} := \frac{1,19\ \frac{PLN}{kW\ hr}}{24,94\ \frac{€}{GJ}} = 3,1$$

That is entirely probable to teach the value of COP. Heat pump utilisation might not be required due to relatively low power needs (460 kW) compared to the HOCLOOP unit (1.6 MW).

Based on previous results, the optimal flow rate per single HOCLOOP unit was estimated to be 20 m³/h of water (working fluid).

With the working fluid flow rate circulating in the HOCLOOP module established in the previous stage of work, optimisation may concern the number of modules. Each additional module will increase the power supplied, but the user's needs will limit the possibility of its use. It will generate additional investment outlays, and the optimal number of HOCLOOP modules will be one of the optimised factors. It was assumed that the optimised objective function would be the payback time of the investment outlays for the additional infrastructure. Additionally, some financial factors commonly used in economic estimation, such as IRR and NPV, will be presented.

This project has received funding from the European Union's Horizon Europe research and innovation program under grant agreement No 101083558

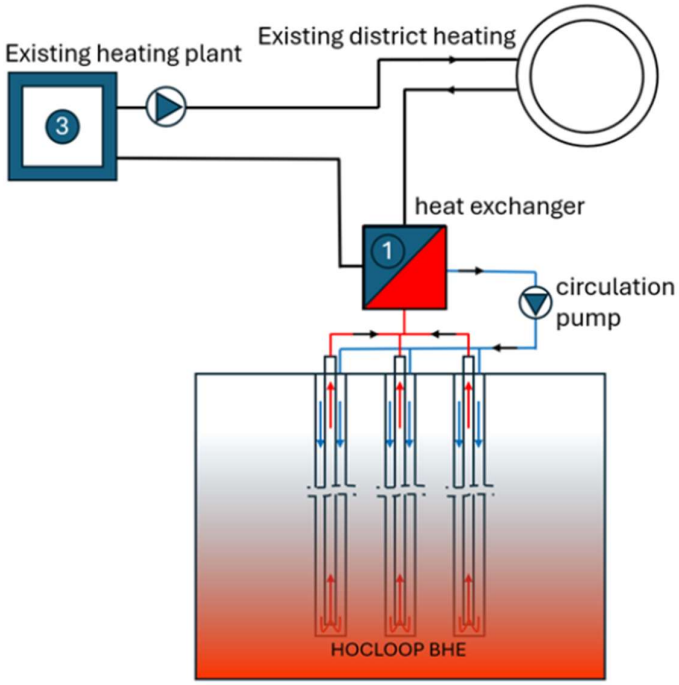

Figure 35. The general scheme of the system utilized the HOCLOOP units without heat pump utilization.

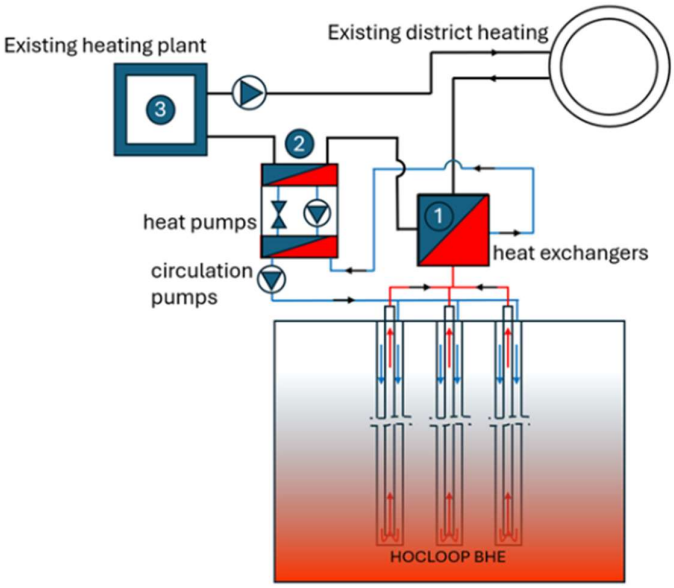

Figure 36. The scheme of the HOCLOOP system supplemented by a heat pump unit.

Finally, the following variants were examined:

- SDhpDEX[n] or SDhpHP[n] - utilisation of the salt dome, obtained energy from the heating plant by a direct heat exchanger DEX (linked with HOCLOOP) and heat pumps HP – if preferable. Utilisation of n HOCLOOP borehole heat exchangers,
- SPhpHP[n] - HOCLOOP units utilise the energy from the salt pillow, and the heating plant uses the obtained energy through a direct heat exchanger and heat pumps, as an option. Utilisation of n units of HOCLOOP,

This project has received funding from the European Union's Horizon Europe research and innovation program under grant agreement No 101083558

- **SPap[n]** - HOCLOOP units utilise the energy from the salt pillow, which is used to heat the Goleniów Airport. A direct heat exchanger linked to HOCLOOP units and optionally heat pumps is used - utilisation of n units of HOCLOOP.

The time length of economic analysis was 30 years in all cases. The authors of this survey predict the significant impact of the connection pipeline on the economic factors. To estimate the influence of the pipeline, there are variants that exclude it from technical and financial analyses. Those variants are marked by the letter "b" at the end of the short variant description, e.g. SDhpDEX1b.

In the case of the Airport, different lengths of the horizontal part of the HOCLOOP borehole heat exchanger are considered: 2 000 m and 500 m. Due to that, in the case of this variant, additional information in the short label of the variant is used: SPapDEX1_2000m and SPapDEX1_500m. In this case, utilisation of heat pumps is unnecessary; the HOCLOOP can cover all power needs in the case of SPapDEX1_2000m, and in the case of SPapDEX1_500m, only a small amount of additional power is needed. It is assumed that it will be supplied by the existing gas-fired heating plant.

Thermal characteristics of district heating in Goleniów are shown in Figure 37, Figure 38, and Figure 39, as well as characteristics of the Airport in Goleniów in Figure 40 and Figure 41.

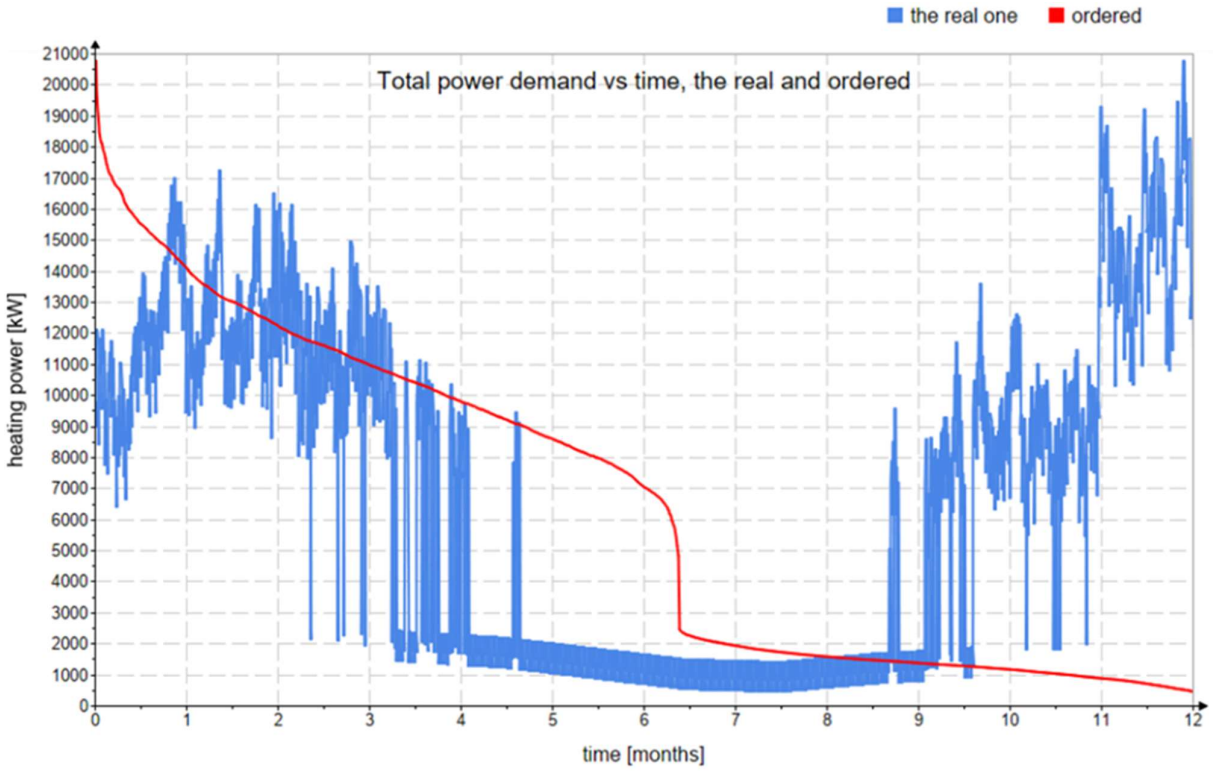

Figure 37. Power demand curves in the case of Goleniów district heating (the result of mathematical model, based on TMY).

This project has received funding from the European Union's Horizon Europe research and innovation program under grant agreement No 101083558

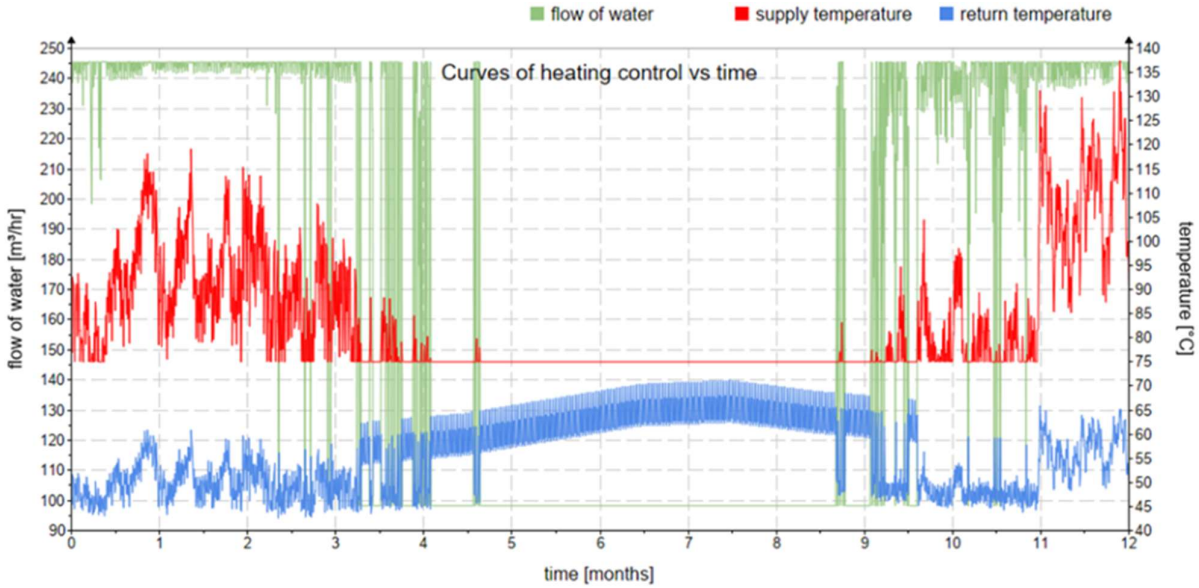

Figure 38. Power control parameters variation in the case of Goleniów district heating (result of mathematical model, based on TMY).

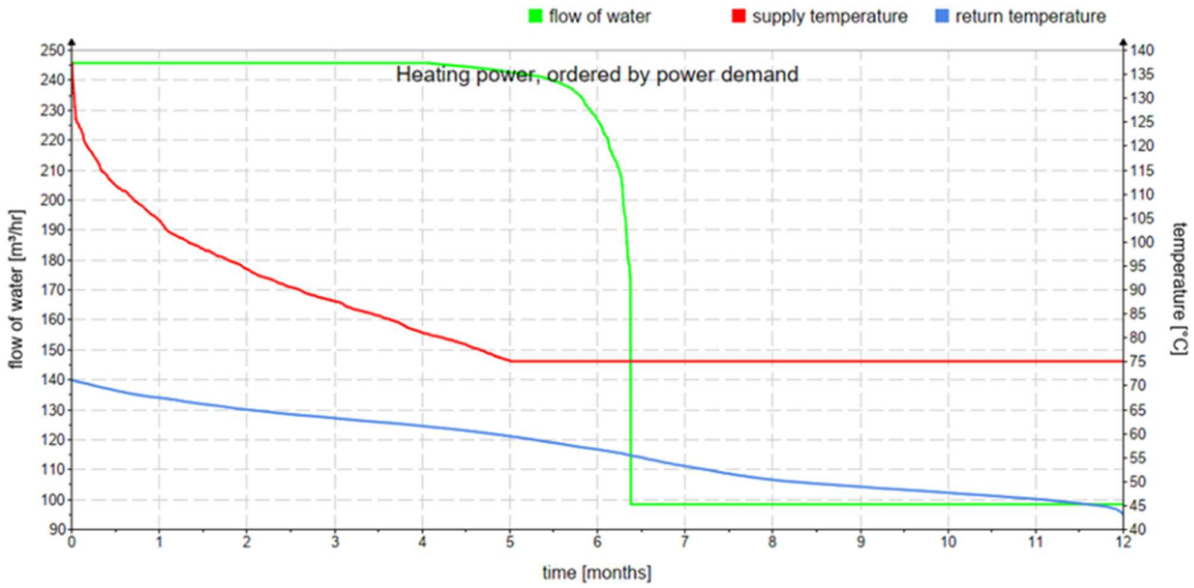

Figure 39. Ordered power control parameters variation in the case of Goleniów district heating (result of mathematical model, based on TMY).

This project has received funding from the European Union's Horizon Europe research and innovation program under grant agreement No 101083558

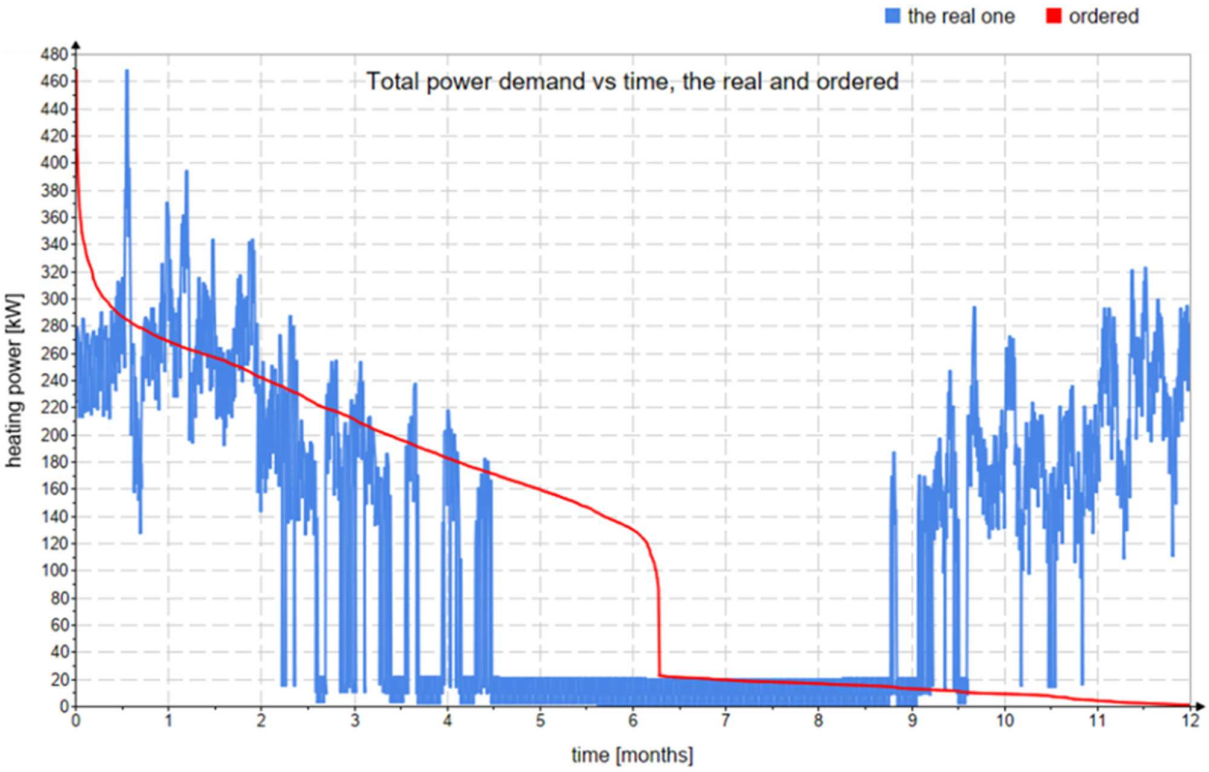

Figure 40. Power demand curves in the case of airport Goleniów (the result of mathematical model, based on TMY).

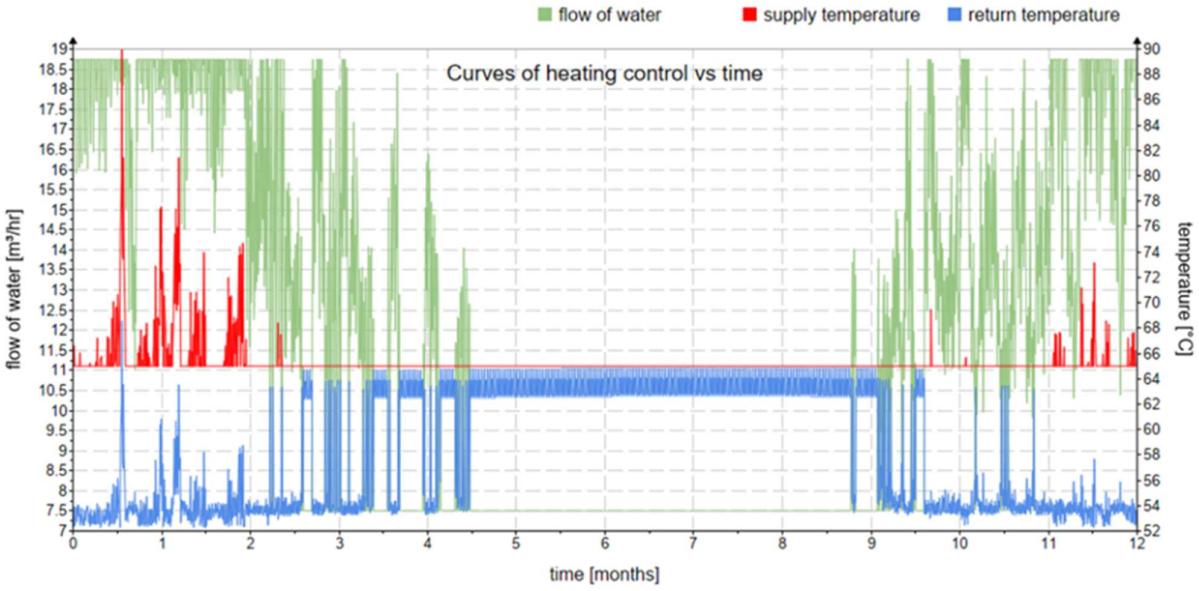

Figure 41. Power control parameters variation in the case of airport Goleniów (result of mathematical model, based on TMY).

3.5.4. Cost analysis

Selected factors describing the working conditions and results in Table 22 are concluded. The table includes an additional variant called SDfitHPb – it refers to an energy consumer who can fully utilise the potential of a single HOCLOOP heat exchanger, drawing energy from a salt dome. This variant is designated SDfitHPb, meaning it does not require a long connection section to the district heating network. It is

This project has received funding from the European Union's Horizon Europe research and innovation program under grant agreement No 101083558

assumed that this consumer will be a hypothetical consumer currently using energy from a hard coal-fired heat source linked to a district heating network. This consumer will disconnect from the district heating network and use energy from a single HOCLOOP module, using heat pumps and a direct heat exchanger. The current reference price of thermal energy is typical for a district heating network, including energy generation and transmission fees. It is assumed to be PLN 152/GJ, i.e., €35.71/GJ net. The heating system of this user is designed for 90/70°C (typical parameters in the case of an existing heating system in Poland). Hot tap water is designed to 65/40°C, typical of a moderate-sized heating system—power requirements: 3 MW for heating and 200 kW for hot tap water.

Effects for all variants were calculated based on the same algorithm. Below are shown some results for SDfitHPb.

Table 22. Summary of selected results for the analysed variants, taking into account technical, energy and economic indicators (results of calculations, based on numerical simulation of HOCLOOP unit conditions).

	Factor\Variant	SDfuDD1	SDfuDD1b	SDfuDD2	SDfuDD2b	SDfuHP1	SDfuHP1b	SDfuHP2	SDfuHP2b	SPfuDD1	SPfuDD1b	SPfuDD2	SPfuDD2b	SPfuHP1	SPfuHP1b	SPfuHP2	SPfuHP2b	SPfuDEX1_100m	SPfuDEX1_500m	SDfitHPb
2	Number of HOCLOOP units [-]	1	1	2	2	1	1	2	2	1	1	2	2	1	1	2	2	1	1	1
3	Length of single HOCLOOP unit [m]	7012	7012	7012	7012	7012	7012	7012	7012	6012	6012	6012	6012	6012	6012	6012	6012	6012	5012	7012
4	Length of horizontal part [m]	2500	2500	2500	2500	2500	2500	2500	2500	2000	2000	2000	2000	2000	2000	2000	2000	2000	500	2500
5	Cost of HOCLOOP unit [k€]	21591	21591	43182	43182	21591	21591	43182	43182	20195	20195	40389	40389	20195	20195	40390	40390	20195	19064	21591
6																				
7	Connection pipeline length [km]	10	0	10	0	10	0	10	0	4,0	0	4,0	0	4,0	0	4,0	0	0	0	0
8	Temperature losses hot/cold [K]	6,7 / 3,3	-/-	3,6 / 1,8	-/-	6,7 / 3,3	-/-	3,7 / 0,5	-/-	1,8 / 0,6	-/-	1,0 / 0,6	-/-	1,8 / 0,6	-/-	1,8 / 0,1	-/-	-/-	-/-	-/-
9	Pressure losses hot/cold [bar]	8,8 / 9,2	-/-	5,9 / 6,2	-/-	8,8 / 9,2	-/-	5,9 / 6,5	-/-	2,4 / 2,5	-/-	1,6 / 1,6	-/-	2,4 / 2,5	-/-	1,6 / 1,7	-/-	-/-	-/-	-/-
10	Investment expenditures for pipeline (2 pre-insulated pipes) [k€]	2736	0	3337	0	2736	0	3337	0	730	0	889,9	0	730	0	890	0	0	0	0
11	Electric power total (HOCLOOP units / connection pipelines) [kW] (negative value means surplus)	8,5(-6,8/17,1)	-6,8(-6,8/6,8)	8,5(7,9/8,4)	7,9(7,9/6,8)	8,5(-6,8/17,1)	-6,8(-6,8/6,8)	8,7(7,9/8,8)	7,9(7,9/6,8)	-0,9(-6,8/5,4)	-6,8(-6,8/6,8)	-0,7(7,9/7,7)	7,9(7,9/6,8)	-0,9(-6,8/5,4)	-6,8(-6,8/6,8)	-10,8(17,7/7,7)	17,7(17,7/6,8)	-6,4(-6,8/6,8)	-5,9(-3,9/6,8)	-6,8(-6,8/6,8)
12																				
13	Direct heat exchanger cost [k€]	46,6	78,8	110	158	50,1	78,4	106,7	115	55	75,7	157,1	150,3	52,4	75,1	106	158,1	22,3	19,20	68,7
14	Direct heat exchanger power [kW]	1055	1674	2335	3348	1064	1666	2268	2440	1165	1610	3339	3196	1113	1600	2314	3361	475	409	1460
15	Heat pumps cost [k€]	0	0	0	0	681	681	1329	1312	0	0	0	0	681	681	1335	1330	0	0	1095
16	Heat pumps heating power [kW]	0	0	0	0	1595	1595	3137	3095	0	0	0	0	1595	1595	3153	3140	0	0	2585
17	Total investments [k€]	24377	21579	48629	43340	25058	22350	47955	44909	20980	20775	41436	40548	21958	20955	42771	41878,1	20717	19023	22755
18																				
19	Power utilised from peak source [kW]	20267	20103	19492	19306	18864	18574	16457	16383	20146	20145	19825	19479	18644	18647	16929	16462	0	239	0
20	Energy production [GJ/year]	304389	304389	304389	304389	304389	304389	304389	304389	304389	304389	304389	304389	304389	304389	304389	304389	3035	3035	29664
21	Average share of direct heat exchangers [-] (average in 30 years)	0,119	0,143	0,252	0,771	0,119	0,144	0,254	0,298	0,129	0,135	0,250	0,26	0,131	0,137	0,253	0,257	1	0,909	0,557
22	Average share of heat pumps [-] (average in 30 years)	0	0	0	0	0,135	0,135	0,178	0,175	0	0	0	0	0,13	0,127	0,177	0,176	0	0	0,343
23	Average share of peak heat source [-] (average in 30 years)	0,881	0,857	0,748	0,729	0,744	0,721	0,571	0,557	0,871	0,866	0,745	0,74	0,739	0,726	0,57	0,566	0	0,011	0
24	Price of energy originated from peak source [€/GJ]	14,53	14,53	14,53	14,53	14,53	14,53	14,53	14,53	14,53	14,53	14,53	14,53	14,53	14,53	14,53	14,53	0	24,94	30,71
25																				
26	Variable price of energy after HOCLOOP utilisation [€/GJ]	12,49	12,49	10,92	10,66	13,77	13,32	12,14	12,2	12,7	12,61	10,9	10,81	13,57	13,45	12,29	12,28	24,94	0,31	5,91
27	Simple payback time [years]	56,5	51,9	93,3	54,6	161	90,4	163,4	93,4	56,1	51,6	55,7	53,4	110,7	95	93,4	90,89	353,5	165,3	28,6
28	NPV(@-0.5%) after 30 years of system exploitation [k€]	<0	<0	<0	<0	<0	<0	<0	<0	<0	<0	<0	<0	<0	<0	<0	<0	<0	<0	<0
29	IRR [-]	<0	<0	<0	<0	<0	<0	<0	<0	<0	<0	<0	<0	<0	<0	<0	<0	<0	<0	<0
30																				
31	Required subsidy ratio to HOCLOOP allows to obtain NPV ~=0 €, after 30 years, discount rate @-5%/yr [-]	0,827	0,7	0,815	0,718	1	0,85	0,945	0,86	0,75	0,7	0,74	0,71	0,82	0,865	0,885	0,86	0,93	0,91	0,5
32	Subsidy amount [k€]	17856	15114	35150	31005	21591	18352	40807	37137	15146	14137	29888	28676	18029	17469	36745	34726	18731	14464	10796
33	SPBT financial expenditures excluding subsidy [years]	15,5	15,7	15,5	15,5	22,3	16,1	15,3	15,7	15,6	15,6	15,6	15,6	15,7	15,8	15,4	15,5	14,6	15,1	15
34																				
35	Additional comments and information					Financial savings are not able to pay back the cost of connection pipe. It is impossible to reach <15 years of simple payback time														

This project has received funding from the European Union's Horizon Europe research and innovation program under grant agreement No 101083558

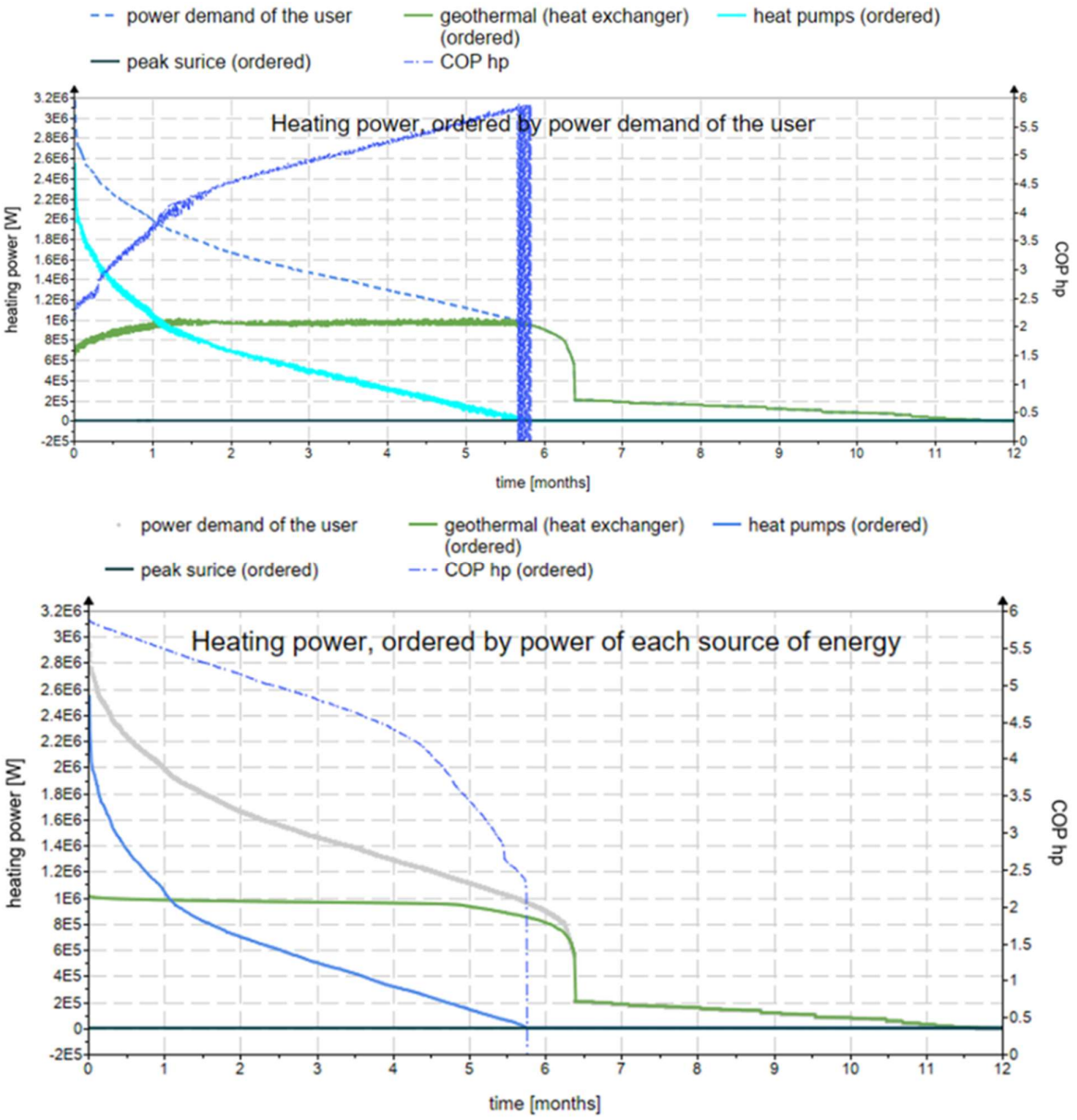

Figure 42. Diagram of covering the power demand with energy sources for the SDfirHPb variant, at the top the graph is ordered by power demand, at the bottom the graph is ordered by power for each of the analysed sources separately. In the 10th year.

This project has received funding from the European Union's Horizon Europe research and innovation program under grant agreement No 101083558

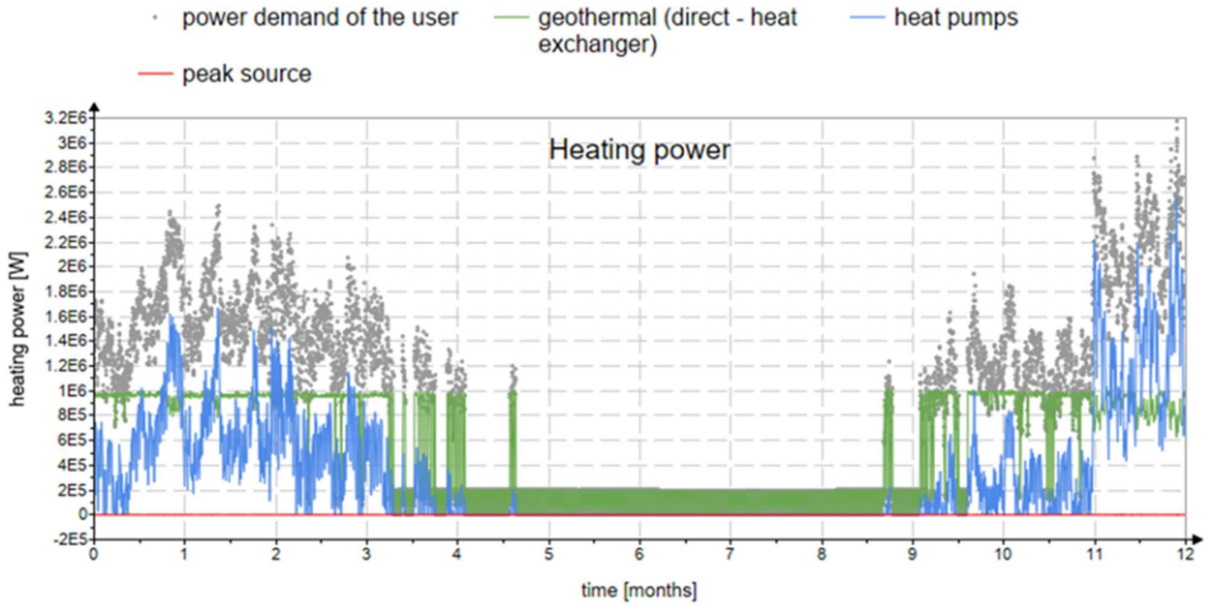

Figure 43. Diagram of covering the power demand for SDfitHPb unordered, the real. In the 10th year of system exploitation.

3.5.5. Discussion

Unfortunately, after analysing the results, it must be concluded that none of the analysed variants is economically viable compared to the heating system currently used in Goleniów. Even the hypothetical SDfitHPb variant is characterised by negative values of the dynamic investment profitability indicators, i.e., NPV and IRR. It was assumed that a variant can be considered economically viable if it is characterised by positive NPV, assuming a discount rate of 5%/year, which is slightly higher than the annual inflation rate in Poland (year-on-year from June 2024 to June 2025, it was 4.1% [33]). Analysing the economic effects, it was decided to test the influence of a subsidy threshold for the HOCLOOP system that would guarantee economic profitability over 30 years of system operation (line 31 in the table). The subsidy threshold was defined as a fraction of the capital expenditures planned to construct HOCLOOP BHE, excluding other cost components (heat exchangers, pipelines, heat pumps, etc.). The subsidy level is also given as an amount in line 32. In line 33, the value of the simple payback time SPBT for the money invested in the whole system, excluding the subsidy. Reached values of SPBT allow for positive NPV after 30 years of energy source operation, assuming a discount rate of 5%/year.

Achieving favourable discount rates for assessing the profitability of the investment in the analysed case is extremely difficult, taking into account the extremely high level of initial investment outlays and the marginalisation of profits achieved over time, in the form of a decrease in the variable costs of energy production. For example, the HOCLOOP, located in the preferred zone of a salt dome, with a total length ~ of 7 km, gives thermal power with 1674 kW (Table 22 row 14, variant SDhpDEX1b). Assuming it replaces energy produced from a reasonable range from 14.53 to 35.71 €/GJ working the whole year, SPBT reaches values from 11.4 to 28.1 years:

$$SPBT := \frac{21.591 \cdot 10^6 \cdot €}{1.674 \cdot MW \cdot \begin{bmatrix} 14.53 \\ 35.71 \end{bmatrix} \cdot \frac{€}{10^9 \cdot J}} = \begin{bmatrix} 28.1 \\ 11.4 \end{bmatrix} yr$$

This project has received funding from the European Union's Horizon Europe research and innovation program under grant agreement No 101083558

The suggested range of reference energy prices analysed above is not coincidental. The lower price corresponds to the case in which the HOCLOOP system is integrated into an existing heating network, replacing part of the power generated by the existing energy source. In this case, heat distribution costs remain unchanged, and HOCLOOP only replaces the thermal generation capacity. Additionally, one of the cheaper available variants was considered, for example, the heating plant in Goleniów. The higher energy price corresponds to the variant in which HOCLOOP is locally integrated into a separate heating network, reducing energy transmission and distribution costs. The analysed energy source is still hard coal, but the energy production costs are typical for coal-fired heating plants, higher than in the case of Goleniów.

$$LF_{HOCLOOP} = \frac{\int_0^{\Delta\tau} P_{HOCLOOP}(\tau)\,d\tau}{max\left(P_{HOCLOOP}\right)\cdot\Delta\tau}$$

where:

$LF_{HOCLOOP}$ – load factor of HOCLOOP unit [-],

τ – time [s]

$\Delta\tau$ - analysed time [s],

$P_{HOCLOOP}$ – power of the HOCLOOP vs time [W].

For example, in the case of the best variant analysed above SDfitHP1b (Figure 43) it is equal to 0.54. SPBT of the HOCLOOP unit can be estimated in this case as:

$$SPBT := \frac{21.591 \cdot 10^6 \cdot €}{1.0 \cdot MW \cdot 35.71 \cdot \frac{€}{10^9 \cdot J} \cdot 0.54} = 35.5\ yr$$

Assuming a 50% subsidy, it is reduced to:

$$SPBT := \frac{\frac{1}{2} \cdot 21.591 \cdot 10^6 \cdot €}{1.0 \cdot MW \cdot 35.71 \cdot \frac{€}{10^9 \cdot J} \cdot 0.54} = 17.7\ yr$$

Which is a bit longer than the value in Table 22, row 33. But it does not include savings related to heat pump utilisation

3.5.6. General conclusion

In the final analysis and considering the feasibility of implementing HOCLOOP systems in Poland, it can be concluded that the target energy consumers should be dedicated heating networks, characterised by at least the average energy price applicable to end users. Unfortunately, it appears that this solution must be implemented with the support of subsidies, and the subsidy share guaranteeing the economic viability of the project depends, among other things, on the technical parameters of the recipient's heating system and the reference prices of energy carriers.

This project has received funding from the European Union's Horizon Europe research and innovation program under grant agreement No 101083558

4. Conclusions

The comprehensive techno-economic analysis of HOCLOOP implementation across five European pilot sites reveals both the potential and challenges of deploying horizontal closed-loop geothermal systems in diverse geological and economic contexts. The study demonstrates that while HOCLOOP technology offers significant technical advantages, particularly in terms of environmental sustainability and operational reliability, economic viability remains strongly dependent on site-specific conditions and market factors.

Comparative Energy Cost Analysis

The levelized cost of energy (LCOE) varies substantially across the pilot sites, reflecting differences in geological conditions, drilling costs, and integration opportunities:

- **French case (Fresnes)**: 378.9 €/MWh. The highest cost due to low geothermal gradient and high drilling requirements for horizontal extensions, making it economically challenging compared to the existing doublet system.
- **Belgian case (VITO/Balmatt)**: 152.5 €/MWh (estimated based on 2.7 M€ total investment for 300 kW average output). More competitive due to reuse of existing dry well and direct building heating application with low temperature requirements. A district heating network is needed as the dry well is about 1 km from the buildings to be heated.
- **German case (Darmstadt)**: Not economically viable. Low temperature gradient (2.1°C/100m) and high drilling costs in crystalline rock make HOCLOOP uncompetitive with alternative solutions like MD-BTES with PPR liners.
- **Italian case (Gavorrano):** 268.8 €/MWh. High cost due to high drilling costs in hard formations and high original rock temperature.
- **Italian case (Amiata):** 77.63 - 96.22 €/MWh. Competitive with other technologies due to the lower cost of the wells and high geothermal gradient (122.3°C/km). The increase in power output of ORC does not justify the increase in capital cost.
- **Polish case (Goleniów)**: 52 - 129 €/MWh depending on integration scenario. Favorable geological conditions in salt structures are offset by high capital costs, requiring 40-60% subsidies for economic viability.

The energy cost calculations presented in this study were conducted based on a 20-year project lifetime, which represents a conservative yet standard approach for infrastructure investment analysis. While extending the economic analysis to consider a 50-year project lifetime an admittedly optimistic assumption given the uncertainties inherent in such long-term projections would yield an energy cost approximately 25% lower than the reference case.

Key Success Factors

The analysis identifies critical factors for economically viable HOCLOOP deployment:

1. High geothermal gradients (>3°C/100m) to maximize thermal extraction
2. Favorable drilling conditions to minimize capital costs

This project has received funding from the European Union's Horizon Europe research and innovation program under grant agreement No 101083558

3. Direct integration with low-temperature heating systems (<70°C)
4. Reuse of existing wells or infrastructure where possible
5. Access to renewable energy incentives or carbon pricing mechanisms

Market Positioning

HOCLOOP systems show the greatest promise in niche applications where conventional geothermal is not feasible due to hydrogeological constraints, and where environmental considerations justify premium energy costs. The technology is particularly suited for dedicated heating networks serving energy-efficient buildings with low-temperature requirements, rather than retrofitting existing high-temperature district heating systems.

Recommendations

Future deployment should prioritize sites combining favorable geological conditions with supportive economic frameworks. The high capital intensity of HOCLOOP systems necessitates innovative financing mechanisms, potentially including green bonds, carbon credits, or public-private partnerships. Technological improvements focusing on drilling cost reduction and heat extraction efficiency enhancement will be crucial for improving economic competitiveness.

The study confirms that while HOCLOOP represents a technically viable solution for sustainable geothermal energy extraction, achieving widespread commercial deployment will require continued technological development, strategic site selection, and supportive policy frameworks that recognize the long-term environmental benefits of carbon-free heating systems.

This project has received funding from the European Union's Horizon Europe research and innovation program under grant agreement No 101083558

5. References

[1] M. Singh, C. Souque, D. Liota, D. Fiasci, B. Laenen, V. Harcouët-Menou, P. Wojnarowski and L. Pająk, "Pilot sites data and integration analysis D4.1_V2," HOCLOOP Project 101083558, 2024.

[2] E. Hernandez, J. Pogacnik, V. Leontidis, H. Pham, P. Wojnarowski, L. Pająk, M. Kaczmarczyk, D. Fiaschi, P. Ungar, F. Gigliotti and E. Falchini, "Underground simulations of the HOCLOOP concept at the selected pilot sites," HOCLOOP Project 101083558, 2025.

[3] O. Vestavik and M. Tjelta, "Detailed design of the DHS and," HOCLOOP Project 101083558, 2023.

[4] O. Vestavik, "Manufacturing of the DHS components for," HOCLOOP Project 101083558, 2025.

[5] E. Hernadez, V. Leontidis, M. Wangen and V. Harcouët-Menou, "Benchmark cases," HOCLOOP Project 101083558, 2023.

[6] V. Leontidis, M. Wangen, P. Ungar and D. Fiaschi, "Flow pipe model for fluid circulation," HOCLOOP Project 101083558, 2023.

[7] V. Leontidis, O. Ricois, M. Wangen and E. Hernadez, "Heat flow models for the closed loop system," HOCLOOP Project 101083558, 2023.

[8] V. Leontidis, N. Anand and M. Wangen, "Optimized design for the closed loop geothermal system," HOCLOOP Project 101083558, 2023.

[9] V. Leontidis, M. Wangen, N. Anand and F. Tosto, HOCLOOP Project 101083558, 2024.

[10] X. Zhu and F. Haglind, "Relationship between inclination angle and friction factor of chevron-type plate heat exchangers," *International Journal of Heat and Mass Transfer,* vol. 162, p. 120370, 2020.

[11] S. Kakaç, H. Liu and A. Pramuanjaroenkij, Heat Exchangers: Selection, Rating, and Thermal Design, CRC Press, 2012.

[12] F. Mota, E. Carvalho and M. Ravagnani, "Modeling and Design of Plate Heat Exchanger," in *Heat Transfer: Studies and Applications*, 2015, pp. 165-199.

[13] Alfa Laval, "The theory behind heat transfer: Plate heat exchangers," [Online]. Available: chrome-extension://efaidnbmnnnibpcajpcglclefindmkaj/https://www.alfalaval.com/globalassets/documents/microsites/heating-and-cooling-hub/alfa_laval_heating_and_cooling_hub_the_theory_behind_heat_transfer.pdf. [Accessed 15 09 2025].

[14] A. Chauvel, Manuel d'Evaluation Economique des Procédés, Editions Technip, 2001.

[15] D. Fiaschi, P. Ungar, F. Gigliotti and A. Meana-Fernandez, "Thermo-Economic Analysis of a Geothermal-driven District Heating Network: comparison between a water-based and a CO2-based grid," *Submitted to Applied Thermal Engineering,* 2025.

This project has received funding from the European Union's Horizon Europe research and innovation program under grant agreement No 101083558

[16] P. Ungar, C. Schifflechner, C. Wieland, G. Manfrida and H. Spliethoff, "Thermo-Economic Comparison of CO2 and Water as a Heat Carrier for Long-Distance Heat Transport from Geothermal Sources," in *36th International Conference on Efficiency, Cost, Optimization, Simulation and Environmental Impact of Energy Systems (ECOS 2023)*, Las Palmas De Gran Canaria, Spain, 2023.

[17] B. Adams, J. Ogland-Hand, J. Bielicki, P. Schädle and M. Saar, "Estimating the Geothermal Electricity Generation Potential of Sedimentary Basins Using genGEO (the generalizable GEOthermal techno-economic simulator)," ChemRxiv Preprint, 2021.

[18] U.S. Bureau of Labor Statistics, "Producer Price Index by Industry: Oil and Gas Extraction," [Online]. Available: https://fred.stlouisfed.org/series/PCU21112111.

[19] P. Ungar, "Use of CO2 as working fluid in geothermal systems, PhD Dissertation," Univeristy of Florence, 2024.

[20] R. Turton, R. Bailie, W. Whiting and J. Shaeiwitz, Analysis, synthesis and design of chemical processes, Pearson, 2008.

[21] [Online]. Available: www.geoportal2.pl.

[22] [Online]. Available: https://www.google.com/finance/quote/EUR-PLN?sa=X&ved=2ahUKEwjyl82-r7mNAxWTQ_EDHc7_NIUQmY0JegQIARAs&window=YTD.

[23] [Online]. Available: https://pl.investing.com/commodities/carbon-emissions, access. [Accessed 27 06 2025].

[24] [Online]. Available: https://cieplo.gov.pl/podglad/8c52b959-3112-45ba-bc6d-858537951d2f?assortmentId=908&voivodeshipId=32&districtId=25657&sortDir=ASC&storageType=COMPANY_STORAGE&pageIndex=0. [Accessed 27 06 2025].

[25] [Online]. Available: https://www.mpec.krakow.pl/taryfy-i-cenniki. [Accessed 27 06 2025].

[26] [Online]. Available: https://www.energiadlalodzi.pl/taryfa-i-cenniki/. [Accessed 27 06 2025].

[27] [Online]. Available: https://www.geotermiakolo.pl/strona/13/taryfa-dla-ciepla. [Accessed 27 06 2025].

[28] [Online]. Available: https://www.rachuneo.pl/cena-pradu. [Accessed 28 05 2025].

[29] [Online]. Available: http://www.cena-pradu.pl/mapa.html. [Accessed 28 05 2025].

[30] [Online]. Available: https://www.sunsystem.com.pl/pl/123-rury-preizolowane-stalowe. [Accessed 08 07 2025].

[31] [Online]. Available: (https://www.sunsystem.com.pl/pl/123-rury-preizolowane-stalowe. [Accessed 08 07 2025].

This project has received funding from the European Union's Horizon Europe research and innovation program under grant agreement No 101083558

[32] [Online]. Available: https://www.sunsystem.com.pl/pl/123-rury-preizolowane-stalowe. [Accessed 01 07 2025].

[33] [Online]. Available: https://pl.wikipedia.org/wiki/Port_lotniczy_Szczecin-Goleni%C3%B3w. [Accessed 18 06 2025].

[34] [Online]. Available: https://wszczecinie.pl/lotnisko-w-goleniowie-ma-przejsc-wielomilionowy-remont-w-planach-powiekszenie-sal-odlotow-i-przylotow/46660. [Accessed 18 06 2025].

[35] [Online]. Available: https://pl.tradingeconomics.com/poland/inflation-cpi.

This project has received funding from the European Union's Horizon Europe research and innovation program under grant agreement No 101083558

6. Appendix

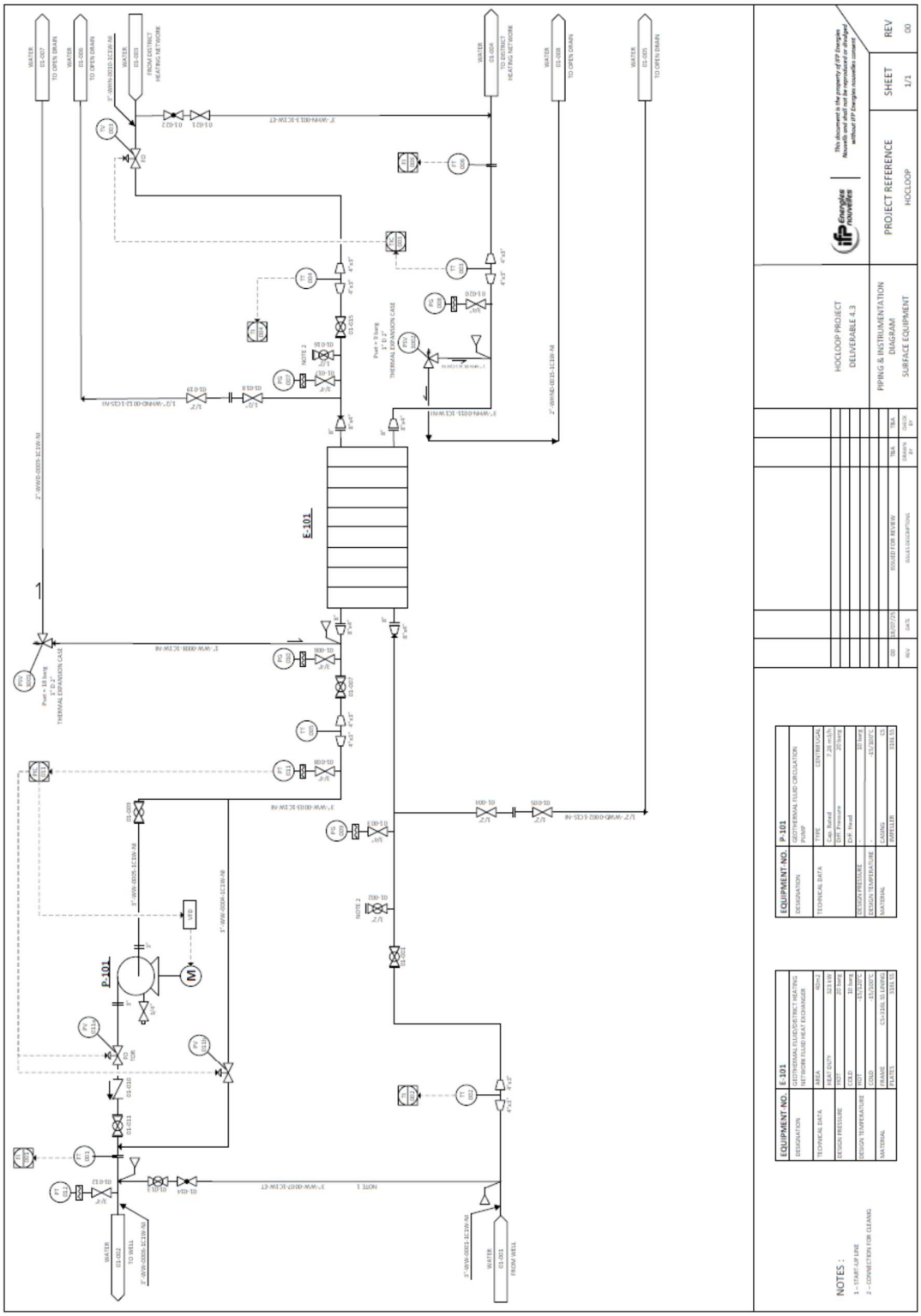

This project has received funding from the European Union's Horizon Europe research and innovation program under grant agreement No 101083558